

1-1-2010

A short cavity fiber laser for microwave and radio-wave generation

Udari M. Basnayaka
Ryerson University

Follow this and additional works at: <http://digitalcommons.ryerson.ca/dissertations>

 Part of the [Electrical and Computer Engineering Commons](#)

Recommended Citation

Basnayaka, Udari M., "A short cavity fiber laser for microwave and radio-wave generation" (2010). *Theses and dissertations*. Paper 825.

This Thesis is brought to you for free and open access by Digital Commons @ Ryerson. It has been accepted for inclusion in Theses and dissertations by an authorized administrator of Digital Commons @ Ryerson. For more information, please contact bcameron@ryerson.ca.

A SHORT CAVITY FIBER LASER FOR MICROWAVE AND RADIO-WAVE GENERATION

by

Udari M. Basnayaka

B.Sc (Eng.), University of Peradeniya, Sri Lanka, 2007

A thesis
presented to Ryerson University
in partial fulfillment of the
requirement for the degree of
Master of Applied Science
in the program of
Electrical and Computer Engineering.

Toronto, Ontario, Canada, 2010

© Udari M. Basnayaka, 2010

Author's Declaration

I hereby declare that I am the sole author of this thesis.

I authorize Ryerson University to lend this thesis to other institutions or individuals for the purpose of scholarly research.

I further authorize Ryerson University to reproduce this thesis by photocopying or by other means, in total or in part, at the request of other institutions or individuals for the purpose of scholarly research.

Instructions on Borrowers

Ryerson University requires the signatures of all persons using or photocopying this thesis. Please sign below, and give address and date.

Abstract

A Short Cavity Fiber Laser for Microwave and Radio-Wave Generation

Udari M. Basnayaka, 2010
Master of Applied Science
Electrical and Computer Engineering
Ryerson University

Broadband and low loss capability of photonics has led to increasing interests in its use for generating, processing, controlling and distributing of microwave and radio-wave signals with low phase noise for applications such as Radio over Fiber systems (RoF), broadband wireless access networks, sensor networks and satellite communiterians.

In this thesis, I have introduced and demonstrated a short cavity Distributed Bragg Reflector (DBR) laser operating in two stable longitudinal modes to generate microwave and radio-wave frequency signals. In the laser, Er/Yb core doped fiber has been used as the gain medium and two wavelength matching fiber Bragg gratings (FBGs) of 99.9% and 90% reflectivity in C-band were used as end reflectors. The dual mode operation was achieved by reducing the cavity length of the fiber laser to 8 mm. It was pumped with a 980 nm pump laser and the laser output has an optical signal-to-noise ratio (SNR) larger than 65 dB at 1533 nm. Due to the birefringence introduced during FBG fabrication two orthogonal polarization modes were observed for each longitudinal mode. Microwave and radio-wave signals were generated by beating these longitudinal and polarization laser modes on a fast photo detector. The generated microwave signals were at 1.2687 GHz, 1.2828 GHz, 14.6962 GHz and 14.7103 GHz with a SNR of 45 dB. The generated radio-wave signals were at 14.1 MHz with a SNR of 30 dB. The 3dB bandwidth of microwave and radio-wave signals were measured to be less than 30 kHz and the Allan variance measurements indicate that the signals are highly stable in frequency. In addition, the generated radio-wave signal is highly stable for temperature variations while the generated microwave signals demonstrated a linear relationship with temperature at 1 MHz/Celsius. Due to high stability of the generated radio-wave signal and low complexity of the overall system this short cavity fiber laser has potential applications such as ultrasonic sensors and optical clocks.

Acknowledgments

I would like to convey my deepest gratitude to my supervisors Dr. X. Gu and Dr. X.N. Fernando for their continuous guidance, encouragement and financial support throughout the project. This thesis would not have been possible without their supports.

I was very fortunate to work with Dr. Gu because his expertise always helped me to improve my knowledge in many fiber optic devices and techniques. Also I admire the patience and endless supports of Dr. Fernando, during the whole period of studies at Ryerson.

Also I convey my heartfelt thank to my family specially my mother, father and my husband for encouraging me and providing me with personal support during my studies.

I would like to thank School of Graduate Studies for providing Ryerson Graduate Award. Last but not least, I would like to thank the Department of Electrical and Computer Engineering for providing me with a unique setting in Fiber Optic Communication and Sensing Lab and Ryerson Communication Lab to carry out my research.

Contents

1	Introduction	1
1.1	Microwave/Radio-Wave over Fiber Systems	2
1.2	Optically Generating Microwave/Radio-Wave Signals	5
1.2.1	Optical Injection Locking	6
1.2.2	Optical Phase Lock Loop	7
1.2.3	External Modulation Method	9
1.2.4	Dual Wavelength Fiber Lasers	10
1.3	Contributions of this Thesis	11
1.4	Outline of the Thesis	12
2	Background and Analysis of Fiber Lasers	13
2.1	Light Sources for Optical Communication	13
2.1.1	Laser Diodes	14
2.1.2	Erbium Doped Fiber Lasers	18
2.2	Fiber Bragg Gratings	20
2.2.1	Hydrogen Loading	22
2.2.2	FBG Fabrication Methods	22
2.2.3	FBG Characteristics	25
3	Laser Fabrication and Experimental Results	26
3.1	DBR Laser Fabrication	26
3.2	Optical Features of the Fiber Laser	29
3.2.1	Dual Longitudinal Mode Operation	30
3.2.2	Orthogonal Polarization Modes	30
3.3	Microwave and Radio-Wave Signal Generation	33
3.3.1	Microwave Signals at 1.2687 GHz and 1.2828 GHz	34
3.3.2	Microwave Signals at 14.6962 GHz and 14.7103 GHz	35
3.3.3	Radio-Wave Signal at 14.1 MHz	36
3.3.4	Beating Effects and 3 dB Bandwidth of Millimeter Waves	37
3.4	Stability Measurements	38
3.4.1	Allen Variance Measurements.	38
3.4.2	Temperature Dependency Measurements	42

3.4.3	Strain Dependency Measurements	44
4	Discussion and Future Works	46
4.1	Possible Other Applications	46
4.1.1	Optical Clockwork	46
4.1.2	Measuring Ultrasound Signals	47
4.1.3	Temperature Sensing	48
4.1.4	Strain Measurements	48
4.2	Conclusion	48
4.3	Future Works	49
	Bibliography	50

List of Figures

1.1	Antenna Remoting in Satellite Communication.	3
1.2	RoF Based Wireless Access System.	4
1.3	Optical Injection Locking of Two Slave Lasers.	7
1.4	Schematic of an Optical Phase Lock Loop.	8
1.5	Microwave Signal Generation Using an MZM.	9
1.6	Dual-wavelength Single Longitudinal Mode Fiber Ring Laser.	10
2.1	The Three Key Processes in Laser Action.	15
2.2	Energy Levels of Er^{+3} Ions.	19
2.3	DBR and DFB Fiber Lasers.	20
2.4	Fiber Bragg Grating.	21
2.5	UV Radiation Over a Phase Mask with Normal Incidence	23
2.6	A Scheme of Phase Mask Utilized in Inscribing FBG	24
3.1	The Experimental Setup for Inscribing Bragg Gratings with a Phase Mask.	27
3.2	The Experimental Setup to Facilitate Laser Pumping and Gain Monitoring. (a). High Reflectivity Grating Writing (b). Low Reflectivity Grating Writing.	28
3.3	The Transmission Spectrum of Two FBGs After Annealing.	29
3.4	Dual Longitudinal Mode Operation of the Short Cavity Fiber Laser.	30
3.5	Orthogonal Polarization Modes in Each Longitudinal Mode - Transmission Spectrum Analysis.	31
3.6	(a). Calibrating Signal. (b). Two Longitudinal Laser Modes with Two Or- thogonal Polarization Modes.	32
3.7	(a). Microwave Signals Generated at 1.2687 GHz and 1.2828 GHz. (b). Zoomed Signal at 1.2828 GHz	34
3.8	Microwave Signals Generated at 14.6962 GHz and 14.7103 GHz.	35
3.9	(a).The Radio-Wave Signal Generated at 14.1 MHz. (b). Zoomed Signal.	36
3.10	Approximated Diagram of Different Modes of the Short Cavity Fiber Laser in Frequency Domain.	37
3.11	Frequency Variation at averaging time of $0.625\mu\text{s}$	39
3.12	Plot of Allan Variance of the 1.2687 GHz Signal.	40
3.13	Plot of Allan Variance of the 1.2828 GHz Signal.	40
3.14	Plot of Allan Variance of the 14.1 MHz Signal.	41

3.15	Comparison of Frequency Stability with Previous Work Reported.	42
3.16	(a).Frequency Variation of the Two Microwave Signals at 1.2687 GHz and 1.2828 GHz with Temperature. (b). Frequency Variation of the Radio-Wave Signal at 14.1 MHz with Temperature.	43
3.17	(a).Frequency Variation of Two Microwave Signals at 1.2687 GHz and 1.2828 GHz with Micro Strain. (b).Frequency Variation of Radio-Wave Signal at 14.1 MHz with Micro Strain	45

Chapter 1

Introduction

Due to ever increasing demand for personal communication services, wireless systems are expected to support more users with higher bandwidths. The increased requirement for high bandwidth is apparent with bandwidth hungry applications such as High Definition Television (HDTV) and video conferencing. To meet these challenges, future telecommunication systems should be capable of providing high quality voice, data and video services to their users at low cost. Integrating the existing and newly deploying telecommunication networks with optical fiber transmission systems is a good idea to cater the demand.

For example, RoF schemes, which refer to a technology of transmitting information bearing radio-wave signals over optical fiber links to facilitate wireless access, can be used to address the need for additional bandwidth cost effectively. These types of links are well known for providing high quality multimedia services.

Microwave over Fiber (MOF) systems can be used to introduce foreseen developments of optical fiber communications to analog transmission systems such as Cable Televisions (CATV) networks. In today's world the majority of the telephony and data communication infrastructure is based on digital transmission protocols. However, analog applications are steadily growing as well.

Optical modulation of millimeter waves or generation of millimeter wave capable optical carriers is a basic requirement of both above mentioned technologies. The most popular scheme is direct or indirect modulation of the laser source with a radio-wave or microwave

signal which carries the data to be transmitted. But using a light source which can generate a microwave or radio-wave capable optical carrier will reduce the system complexity significantly and hence the overall cost of the network. Moreover frequency down conversion from optics to microwave or radio-wave can be applied in many other interesting applications such as optical clock, which enables precise measurements of time.

1.1 Microwave/Radio-Wave over Fiber Systems

RoF refers to a technology whereby light is modulated with a radio signal and transmitted over an optical fiber link to the radio access point to facilitate wireless access. It is an optical interface between the central base station and the radio base station. RoF link consists of an optical transmitter which can generate radio-wave capable optical carrier or an internal/external modulation scheme to modulate the data signal in radio frequency domain. The optical receiver system which is located at the radio base station demultiplexes the signal and converts it into electrical signal to be transmitted by using an antenna. The types of fiber can be single mode or multi-mode. The former is popular because of the low loss and low dispersion capabilities. Graded-index multi-mode fibers are used predominantly in applications like local area networks because of their relatively low modal group velocity dispersion and the large fiber core size. There are several notable advantages of RoF links. Optical fiber is an excellent low loss medium allowing the distribution of radio frequency signals over long distance in a broad bandwidth (several THz). Other benefits include light weight, resistance to electromagnetic interferences and flexibility.

Microwave or radio-wave signal sources with low phase noise are desirable for many applications such as radar, wireless communications, software defined radio and modern instrumentation. Frequently, microwave or radio-wave signals are generated with many stages of frequency doubling by using electronic circuitry, which are complicated and costly. Most of the time, the generated signals have to be sent to the remote sites. Transmitting microwave or radio-wave signals in electrical domain is not the best way because of high losses associated

with electrical distribution lines such as coaxial cables. As discussed above, transmitting microwave and radio-wave signals over optical fibers enables using the very broad bandwidth and low loss features of state-of-the-art optical fiber. Therefore generating millimeter wave signals in optical domain will be a good approach to reduce equipment requirements of the overall communication network.

An evidence of this is antenna remoting and surveillance in satellite communication. Microwave signals at 4-8 GHz (C-band in microwave spectrum) and 12-18 GHz (Ku band) are most commonly used by satellite communication systems. Under bad weather conditions, alternate antennas that are located several kilometers away can be used to maintain the link budget as depicted in Figure 1.1. In such scenario the transmitting of microwave signals over an optical fiber link enables to have remote antennas hundreds of kilometers away from the ground stations, which is not practical with microwave transmission systems in electrical domain.

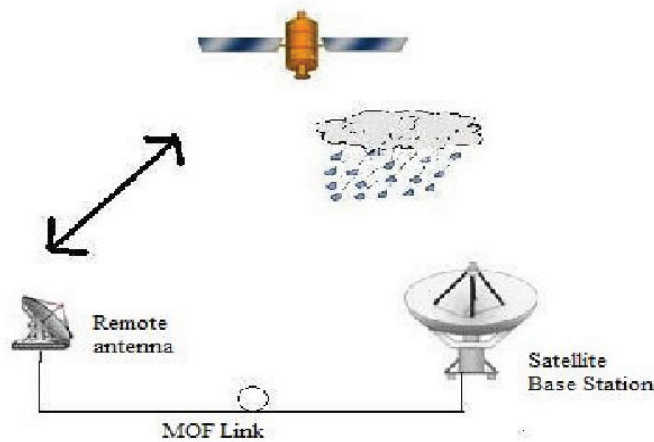


Figure 1.1: Antenna Remoting in Satellite Communication.

Another foreseen evolution in optical generation of microwave signal is providing hot-spot coverage through RoF systems while integrating the 3G and beyond cellular networks with Wireless Local Area Networks (WLANs). Supermarkets, subway stations and airport

concourses are ideal examples for hot-spots. Current WLAN systems operated in 2.4 GHz are capable of providing high speed data rates up to 150 Mb/s.

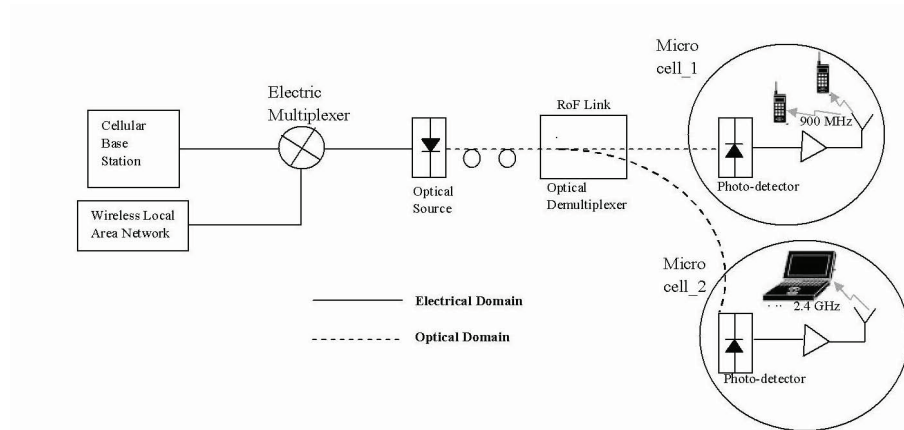


Figure 1.2: RoF Based Wireless Access System.

Figure 1.2 shows a sub carrier multiplexed fiber-to-the-curb wireless down-link which facilitates the transmission of cellular radio-wave signals at 900 MHz as well as WLAN microwave signals at 2.4 GHz. Microwave and radio-wave signals are converted into optical domain and transmitted from the cellular base station to remote wireless devices located in each micro-cell via an optical fiber. The typical radius of a micro-cell is approximately 50-100 meters. The regenerated microwave or radio-wave signal at the radio access point is retransmitted to the remote wireless devices wirelessly within this distance. The radio access point consists of simple devices to convert optical signals into electric signals and vice versa. It serves as an extended antenna from the cellular base station. In such systems high data rates are possible with reduced bit error rates because of the short air interface.

Generating microwave signals in optical domain is desirable for some areas in telecommunication instrumentation as well. In general large phase array systems and radar signal processing units require time delay elements. The small dimensions in micrometer scale and the low loss capabilities make optical fibers a good candidate for microwave delay lines. This

enables getting delays up to hundreds of microseconds which cannot be easily accomplished by electrical delay lines.

1.2 Optically Generating Microwave/Radio-Wave Signals

A microwave or radio-wave signal can be generated optically by using optical heterodyning; by beating of two optical waves of different wavelengths at a photo-detector. The electric beat note generated at the photo-detector corresponds to the wavelength separation of the two signals.

With this approach microwave and radio-wave signals can be generated up to THz band; only limited by the bandwidth of the photo-detector. But by beating two optical signals from two free running laser diodes would lead to microwave or radio-wave signal with high phase noise since the phase of the two optical waves are not correlated each other.

Number of techniques have been introduced and demonstrated during recent years to generate microwave and radio-wave signals with reduced phase noise. These methods can be classified into four main categories.

1. Optical Injection Locking.
2. Optical Phase Lock Loop.
3. Microwave Generation based on External Modulation.
4. Dual Wavelength Fiber Lasers.

This thesis is mainly focused on generating microwave/radio-wave signals using dual wavelength fiber lasers; the last method mentioned above.

1.2.1 Optical Injection Locking

J. Genest *et al.* have demonstrated a method to generate microwave signals by beating two optical signals generated from a single laser diode in [1]. The phase coherence of two laser beams has been achieved by using optical injection locking as depicted in Figure 1.3. The system comprises of one master laser and two slave lasers. The reference signal having a frequency of f_m is applied to the master laser; so that the laser output has an optical carrier frequency signal as well as the side band signals corresponds to the frequency f_m . The signal from the master laser was then fed into the two slave lasers. The two slave lasers have been selected such that their free running frequencies are closer to the sidebands of the output of the master laser; like -1^{st} order and $+1^{st}$ order sideband signals. Thus the optical injection locking can be achieved because, the two lasers are locked to the frequencies corresponds to -1^{st} and $+1^{st}$ sidebands of the modulated signal. The output signals of two slave lasers are coherent in phase because they were locked to the same master laser. So by beating these two optical signals on a photo-detector, a microwave signal having low phase noise can be generated and its frequency is related to the frequency of the modulating signal.

The requirement of an external reference frequency with high stability and difficulties in selecting or tuning the slave lasers to get the frequency locking are the major limitations of this method.

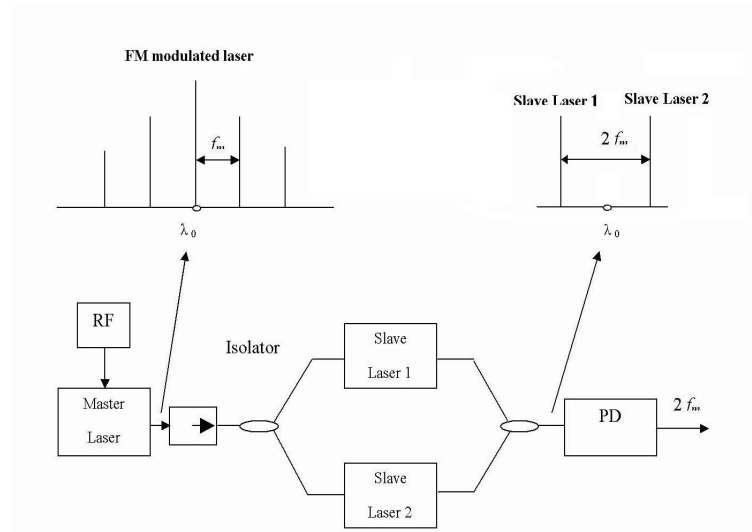


Figure 1.3: Optical Injection Locking of Two Slave Lasers.

1.2.2 Optical Phase Lock Loop

Another approach to generate microwave signals while achieving optical phase coherence is using of an optical phase lock loop. This method has been extensively studied by several groups during past few years[2]-[4]. Here the phase of one laser is actively locked to that of the second laser with the optical phase lock loop.

In [2], a beat note has been generated at the photo-detector by beating of two optical signals from two different external-cavity GaAlAs lasers. Phase of the beat note is compared with that of the external radio frequency reference at a mixer followed by a low pass loop filter as shown in Figure 1.4. The module in the dotted box can be identified as an electrical phase detector, and the output voltage corresponds to the phase difference between the beat note and the radio frequency reference signal. This error voltage is fed back to one of the lasers to control its phase by changing the cavity length or the driving current. With a proper feedback loop gain and response time, the relative phase fluctuations between the two lasers are significantly reduced and the phase of the beat note is locked to the radio frequency reference. For effective phase locking, the two lasers should be selected to have

narrow line widths and therefore have phase fluctuations only at low frequencies, which would ease significantly the requirement of a very short feedback loop.

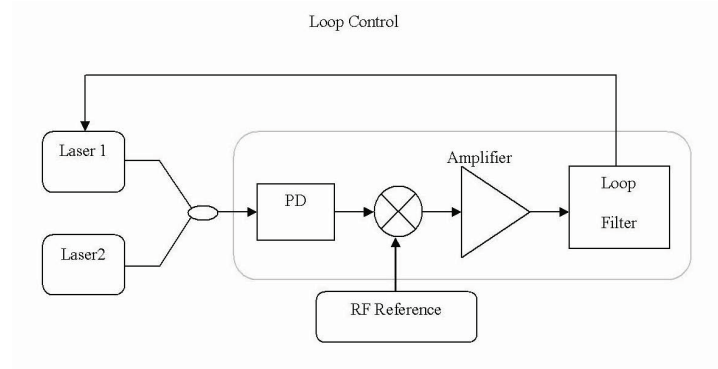


Figure 1.4: Schematic of an Optical Phase Lock Loop.

To increase the frequency acquisition capability, a modified optical phase lock loop that incorporated a frequency discriminator has been proposed in [3].

In [4], dual wavelength Brillouin cavity laser has been used to generate two optical signals to be beaten at the photo detector. Dual mode operation has been achieved by pumping the fiber laser by using two pump lasers with different wavelengths. Two feedback servos have been used to get the phase locking.

As discussed above, in optical phase lock loop method, the two optical signals to be beaten at the photo-detector were generated by using two different laser diodes. External feedback mechanisms have been occupied to get the phase coherence and this makes the overall system more complicated.

1.2.3 External Modulation Method

High quality microwave signals can be generated base on external modulation; by using external modulators like Mach-Zehnder Modulators (MZMs) [5]-[6]. In [5], a frequency doubled optical signal has been generated by biasing the MZM to suppress even order optical sidebands. A 36 GHz signal was generated by driving the modulator with a signal having a frequency of 18 GHz. The simplified schematic diagram of another approach, to generate continuously tunable microwave signals introduced in [6], is indicated in Figure1.5. The system consists of a MZM biased at the maximum bias point of its transfer function to suppress the odd order optical side bands. A wavelength fixed notch filter was used to filter-out the optical carrier. A stable, low-phase noise microwave signal was generated having a frequency of four times that of the radio frequency driving signal.

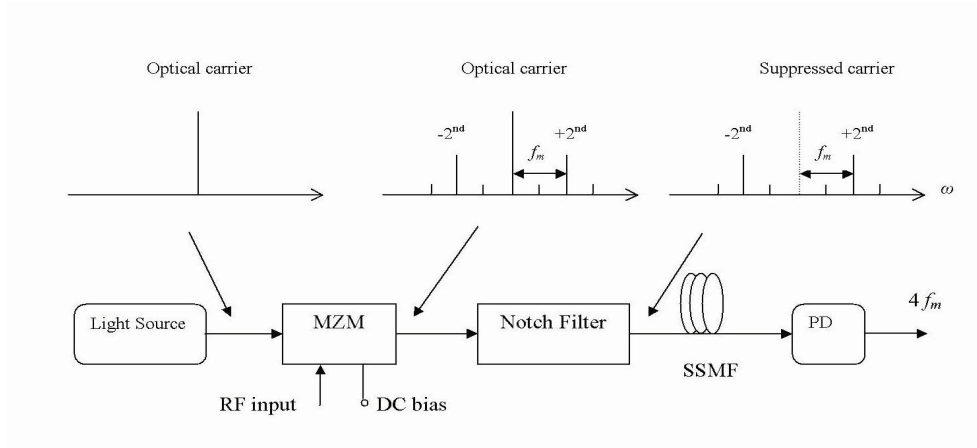


Figure 1.5: Microwave Signal Generation Using an MZM.

Major drawback of this method is the price associated with the MZM.

1.2.4 Dual Wavelength Fiber Lasers

In this method, the two optical signals to be beaten at the photo-detector will be generated by using a single optical source. In many cases the laser source generates a single optical beam with a certain bandwidth and then external mechanisms have been used to split that into two beams [4], [7] and [8]. Here the generated optical signals are not phase locked with each other. But the phase noise of the generated radio-wave or microwave signal is low because both the optical signals are generated by a single source.

X. Chen *et al.* have demonstrated a method to generate microwave signals using a fiber ring laser [7], as shown in Figure 1.6. Ultra-narrow transmission-band dual-wavelength FBG, has been fabricated in combination with a regular FBG, using the equivalent phase shift technique. A semiconductor optical amplifier has been used as the gain medium. The ring laser operates with a single longitudinal modes with two wavelengths. In this method, employing of semiconductor optical amplifier avoids the all-fiber-structure of the laser. Inadequate lasing output power is apparent with the use of an Erbium Doped Fiber Amplifier (EDFA).

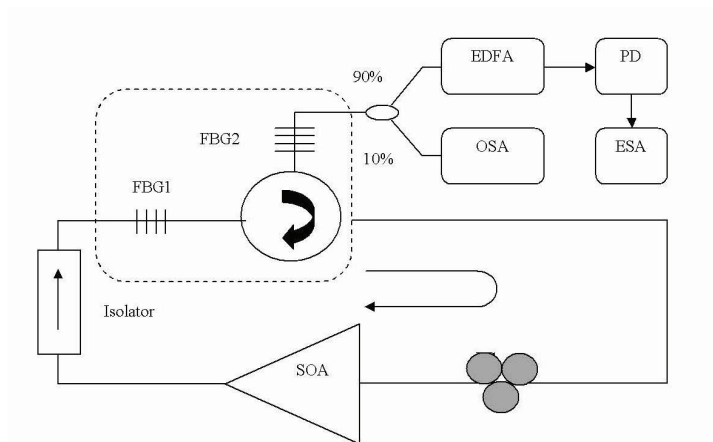


Figure 1.6: Dual-wavelength Single Longitudinal Mode Fiber Ring Laser.

In [8], a micro-ring resonator has been used to get an optical comb profile out of an Erbium doped fiber ring laser. Then a tunable bandpass filter has been used to select two optical modes from the comb profile. Even though the fiber laser alone is not capable of

generating dual wavelength optical output, the overall system gives two optical signals to be beat at the photo-detector. The complexity and the difficulties in fabrication of narrow bandwidth filters are the major limitations of this method.

The experimental setup introduced by Jihong Geng *et al.* consists of a dual frequency Brillouin fiber laser to generate two optical signals [4]. However, since the laser was pumped with two pump lasers, external feedback mechanism has been used to reduce the phase noise of the generated microwave signals.

In [9]-[11] Dr Tam and his group from Hong Kong Polytechnic University have demonstrated a short cavity Er/Yb-doped fiber laser, operating with single longitudinal mode consisting of dual orthogonal polarization modes. It was used to measure the ultrasound signal frequencies. Even though they have generated microwave signals in the range of 1-2 GHz during the experiment, impossibility of down converting the generated microwave signals into lower frequencies is a major limitation.

1.3 Contributions of this Thesis

The major contribution of this thesis is the design, fabrication and the experimental study of a short cavity Er/Yb-doped fiber laser which is capable of down converting the optical frequency into microwave and then to radio-wave. The fabricated fiber laser operates with two stable longitudinal modes and each longitudinal mode consists of two orthogonal polarization modes. The laser can be a perfect candidate for generating microwave and radio-wave capable optical carriers. Series of experiments were performed to visualize the different modes of the laser output. The stability of the generated microwave/radio-wave signals is verified by using Allan variance measurements. Temperature and strain effects on the microwave and radio-wave signals were also investigated.

1.4 Outline of the Thesis

The remainder of this thesis can be summarized as follows:

Chapter 2: This chapter describes the fundamentals of fiber lasers and FBGs with a special attention towards their mathematical relationships. Er/Yb co-doped fiber laser as well as different FBG fabrication methodologies has been discussed in detail.

Chapter 3: This chapter mainly focuses on the fabrication process and the experimental results of the short cavity fiber laser. Two different methods which were used to measure the longitudinal modes and the orthogonal polarization modes has been discussed in detail. Then the characteristics of the generated microwave/radio-wave signals have been discussed, while realizing the beating effect of each signal. Finally the results of Allan variance measurements, temperature and strain stability measurements are presented.

Chapter 4: In this chapter, other possible applications of this short cavity fiber laser, like optical clockworks, measuring ultrasound signals, temperature sensing, strain measurements have been discussed. Conclusion summarizes the overall experimental procedure and the final results. The last subsection of the chapter details possible improvements and the future works of this experimental work.

Chapter 2

Background and Analysis of Fiber Lasers

This chapter details the theoretical background of the thesis. First the laser concepts to obtain dual longitudinal mode operation as well as mathematical description of FBGs have been discussed. Then the FBG fabrication process has been discussed in detail.

2.1 Light Sources for Optical Communication

In choosing an optical source for any kind of optical transmission system, various characteristics of the fiber, such as geometry, attenuation as a function of wavelength, group delay distortion (bandwidth), and its modal characteristics, must be taken into account. In general the following characteristics are applicable for any optical source which can be used for optical communications.

- The amount of light that can be coupled into the fiber depends on its core diameter and Numerical Aperture (NA). So, the optical sources with narrow radiation patterns are preferred to launch enough light into fiber guides having low NA.
- Capability for generating and coupling adequate amount of output power into the fiber enables to achieve longer distances without repeaters.
- Fast response time of the optical source (wide band capability) enables high speed communication links.

- Having a narrow line-width is preferable to reduce dispersion losses in the system.
- Finally they should be reliable, simple in structure and cost effective to be used in real world applications.

Two different kinds of optical sources are exclusively used in optical communication namely heterojunction-structured semiconductor laser diodes (also referred as Injection Laser Diodes or ILDs) and Light Emitting Diodes (LED). Due to spatial and temporal coherence, narrow line width, narrow bandwidth and high power output, laser diodes have become popular in long haul communication systems with high data rates. However the high cost compared to the LEDs is a major drawback.

2.1.1 Laser Diodes

The principle of operation of lasers can be identified under three main processes: photon absorption, spontaneous emission and stimulated emission. These three processes are indicated in the simple two-energy level diagram in Figure 2.1, where, E_1 is the ground state energy and the E_2 is the excited state energy. According to Plank's law, a transition between these two states involves the absorption or emission of a photon having energy of $h\nu_{12} = E_2 - E_1$.

Normally the system is in ground state. When a photon of energy $h\nu_{12}$ impinges on the gain medium, an electron in state E_1 can absorb the photon energy and be excited into state E_2 . Since this is an unstable state, the electron will return back to the ground state soon there by emitting photon of energy $h\nu_{12}$. This happens without any external stimulation, and is called spontaneous emission. These emissions are isotropic and of random phase, and thus appear as a narrow-band Gaussian noise output. The electron can also be induced to make a downward transition from the excited level to the ground-state level by an external stimulation. As shown in Figure 2.1-c if a photon of energy $h\nu_{12}$ impinges on an electron which is in its excited state, the electron will be immediately stimulated to drop to the ground state and give a photon of energy $h\nu_{12}$. This emitted photon is in phase with the incident photon, and the resulted emission is called stimulated emission.

In thermal equilibrium the density of excited electrons is very small. Most photons incident on the gain medium will therefore be absorbed, so that the stimulated emission is essentially negligible. Stimulated emission will exceed absorption only if the population of the excited state is greater than that of the ground level. This is known as population inversion. Since this is not an equilibrium condition, population inversion is achieved by various pumping techniques.

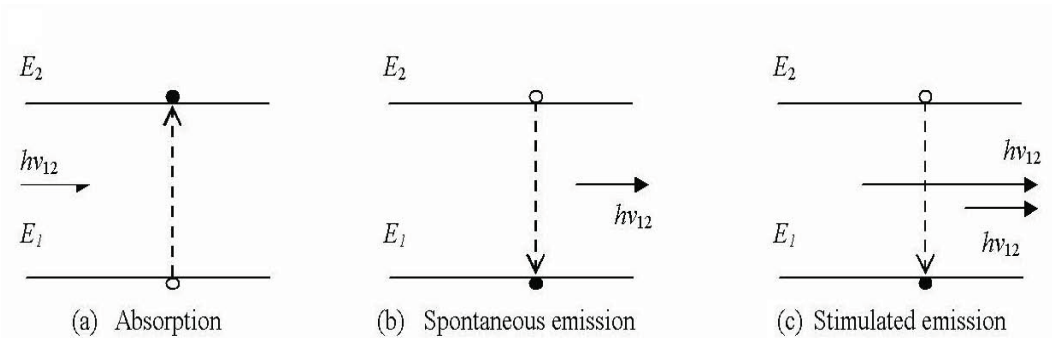


Figure 2.1: The Three Key Processes in Laser Action.

In laser diode, a pair of flat, partially reflecting mirrors are directed toward each other to enclose the cavity. The purpose of these mirrors is to provide strong optical feedback in the longitudinal direction, thereby converting the device into an oscillator with a gain mechanism that compensates for optical losses in the cavity. The laser cavity can have many resonance frequencies. The device will oscillate at these resonance frequencies for which the gain is sufficient to overcome the cavity losses. A mathematical model will be discussed to determine the lasing conditions and resonant frequencies, in next few paragraphs.

The electromagnetic wave propagating in longitudinal direction z , can be expressed in terms of electric field phasor as,

$$E(z, t) = I(z)e^{j(\omega t - \beta z)} \quad (2.1)$$

where, $I(z)$ is the optical field intensity, ω is the optical radiation frequency, and β is the

propagation constant.

Lasing is the condition at which light amplification becomes possible in the resonance cavity and to do that the population inversion should be achieved. This condition can be understood by considering the fundamental relationship between $I(Z)$, the absorption coefficient α_λ , and the gain coefficient g in the cavity. The radiation intensity at a photon energy $h\nu$ varies exponentially with the distance z according to the relationship

$$I(z) = I(0)e^{[\Gamma g(h\nu) - \alpha(h\nu)]z} \quad (2.2)$$

where, Γ is the optical-field confinement factor.

Optical amplification of selected modes is provided by the feedback of the optical cavity. In the repeated passes between the two partially reflecting parallel mirrors, a portion of radiation associated with those modes that have the highest optical gain coefficient is retained and further amplified during each trip through the cavity. Lasing occurs when the gain of one or several guided modes is sufficient to exceed the optical losses during one round-trip through the cavity; that is $z=2L$. During the round-trip, only the fractions of R_1 and R_2 of the optical radiation are reflected from the two end mirrors. Due to this, lasing condition in above Eq (2.2) becomes

$$I(2L) = I(0)R_1R_2e^{2L[\Gamma g(h\nu) - \alpha(h\nu)]}. \quad (2.3)$$

At the lasing threshold, a steady state oscillation takes place, and the magnitude and the phase of the returned wave should be equal to those of the original wave so that

$$I(2L) = I(0) \quad (2.4)$$

in magnitude and

$$e^{-j2\beta L} = 1 \quad (2.5)$$

in phase. Here β can be written as

$$\beta = \frac{2\pi n}{\lambda}. \quad (2.6)$$

The condition indicated in above Eq (2.6) holds when

$$2\beta L = 2\pi m \quad (2.7)$$

where, m is an integer. From Eq (2.6) and Eq (2.7)

$$m = \frac{L}{\frac{\lambda}{2n}} = \frac{2Ln}{c}v \quad (2.8)$$

because $c = \nu\lambda$ and this states that the cavity resonates when an integer number m of half wave lengths spans the region between the mirrors.

Since in all lasers, the gain is a function of frequency, there will be a range of frequencies for which Eq (2.8) holds. Each of these frequencies corresponds to a mode of oscillation of the laser. Depending on the laser structure, any number of frequencies can satisfy Eq (2.8). Thus, some lasers are single mode while some are multi-mode.

The frequency spacing of laser modes can be found by considering two successive modes of frequencies ν_{m-1} and ν_m represented by the integers $m-1$ and m . From above Eq (2.8)

$$1 = \frac{2Ln}{c}(\nu_m - \nu_{m-1}) = \frac{2Ln}{c}\Delta\nu \quad (2.9)$$

and frequency spacing can be derived as,

$$\Delta\nu = \frac{c}{2Ln}. \quad (2.10)$$

This can be related to wavelength spacing $\Delta\lambda$ as

$$\Delta\lambda = \frac{\lambda^2}{2Ln}. \quad (2.11)$$

According to Equation 2.11, wavelength separation of longitudinal laser modes is inversely proportional to the cavity length of the laser. So, the frequency of the microwave signal generated by beating of two longitudinal modes of a laser, can be changed by changing the cavity length of the laser.

2.1.2 Erbium Doped Fiber Lasers

In fiber lasers, rare earth doped fibers are used as the gain media. The first rare-earth-doped fiber laser was built over 30 years ago. Since then many doped fiber lasers have been reported with lasing wavelengths from 550 nm to 2900 nm, based on Erbium (Er^{3+}), Ytterbium (Yb^{3+}), Neodymium (Nd^{3+}), Thulium (Tm^{3+}) and Praseodymium (Pr^{3+}) [12].

Optical pumping mechanism and the end reflectors convert the fiber gain medium into a laser resonator. Electrically driven semiconductor laser diodes can be used as pump lasers and dielectric mirrors, dielectric coatings on the fiber ends or FBGs can be used as the end reflectors. The latter is the most popular among commercially available fiber lasers. The pumping wavelength of the fiber laser should be selected by considering the different properties such as emission/absorption cross sectional area, decay time and excited state absorption of different energy levels of the gain medium [12]. For example Er^{3+} can be pumped at 510, 532, 665, 810, 980 and 1480 nm. But last two wavelengths being favored because there is no excited state absorption at these wavelengths.

Erbium as a Gain Medium

Erbium is widely used as a trivalent ion as Er^{3+} and used for both fiber lasers and amplifiers as the gain medium. Energy level structure of trivalent Er^{3+} ion is indicated in Figure 2.2.

The most common laser transition of Erbium is from ${}^4I_{13/2}$ manifold to ground state manifold ${}^4I_{15/2}$, which has a transition wavelength of 1530-1600 nm. The threshold pump power is high because of the quasi-three-level transition. The population inversion and consequently the net laser gain can be achieved only when more than half of the ions are pumped into the upper level.

Even though the in-band pumping is possible in 1450 nm wavelength (${}^4I_{15/2}$ to ${}^4I_{13/2}$) the most common pump is based on the transitions ${}^4I_{15/2}$ to ${}^4I_{11/2}$ at a wavelength of 980 nm, because at this wavelength the emission cross section of the iron is negligible compared to that at 1550 nm [12]. Because the electron life time of ${}^4I_{11/2}$ is about $10 \mu s$, excited electrons tend to transfer to ${}^4I_{13/2}$ quickly. At this level excited state life time of irons is 8-10 ms, so that the population inversion can be achieved at this meta-stable level.

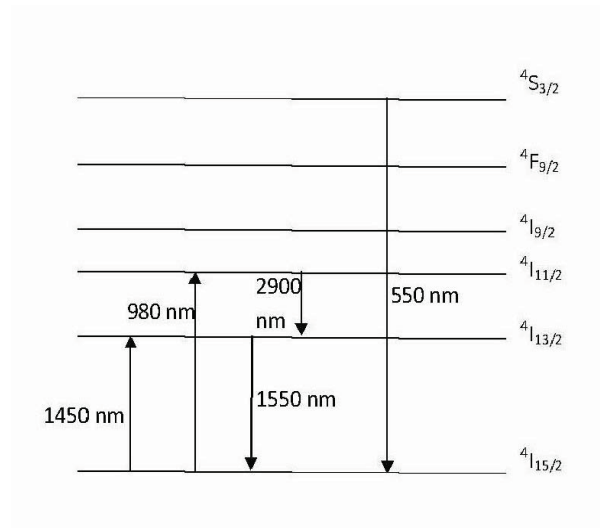


Figure 2.2: Energy Levels of Er^{+3} Ions.

However pumping at the wavelength 980 nm to get the transition of ${}^4I_{15/2}$ to ${}^4I_{11/2}$ is not easy because of the Er^{+3} concentration required is limited by the small absorption area of the fiber core. So in order to increase the absorption at 980 nm the gain medium can be co-doped with Yb^{+3} ions. The ytterbium ions can effectively absorb pump radiations at around 950 nm and then transfer the energy to erbium ions in the ground state manifold to

bring them to ${}^4I_{11/2}$. From that level, the ions are quickly transferred into the upper laser level ${}^4I_{13/2}$, so that the energy transfer back to ytterbium is suppressed.

Two different types of FBG reflected fiber lasers are there namely DBR lasers and Distributed feedback lasers (DFB). In DBR lasers two FBGs which are separated in cavity length, are used as end reflectors. These two wavelength matching FBGs can be identical or can be different from each other in reflectivity and in length. In DFB lasers, only one FBG is there with a 180° of phase shift in the middle as indicated in the figure.

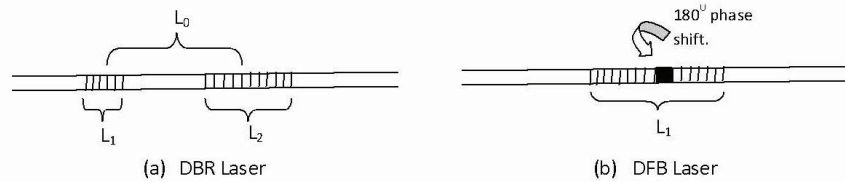


Figure 2.3: DBR and DFB Fiber Lasers.

2.2 Fiber Bragg Gratings

A Fiber Bragg Grating is a structure having a periodic or aperiodic variation of the effective refractive index of the fiber core. Typically the permanent perturbation is periodic over few millimeters or even few centimeters while having a period of about hundred nanometers. Appropriate selection of the length and the period of this corrugated structure will lead to reflect a narrow range of wavelengths, propagating along the fiber, for which the Bragg condition satisfies. The center wavelength of the reflected signal or the Bragg grating wavelength is given by $\lambda_{FBG} = 2\Lambda n_{eff}$ where Λ is the period of the grating pattern and n_{eff} is the effective refractive index. When an optical signal with a certain line-width is transmitted along a FBG, only the wavelength matches to λ_{FBG} will be reflected while all the other wavelengths pass the FBG without any affect.

The formation of permanent gratings in optical fibers was first demonstrated by Hill et al. in 1978 at the Canadian Communication Research Center, Ottawa, Canada. Since then, it has been used for variety of applications in different disciplinarians. FBGs often involves in wavelength filtering in optical communication systems for separating or combining multiple wavelengths for wavelength division multiplex systems. Temperature and strain dependency of FBGs lead to use them in temperature and strain sensing. Also FBGs can be used as end mirrors for fiber lasers. Other foreseen applications of FBGs include dispersion compensation, fiber taps, fiber erbium amplifiers and network monitoring. Advantages of fiber gratings over competing technologies include all fiber geometry, low insertion loss, high return loss and comparatively low cost.

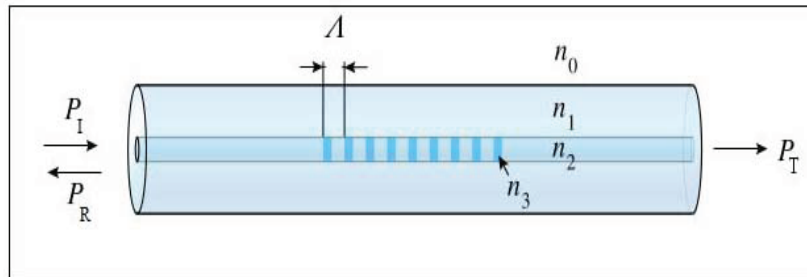


Figure 2.4: Fiber Bragg Grating.

FBGs can be fabricated by exposing the fiber core to an Ultra-Violet laser light (Typically KrF at 248 nm or ArF excimer laser at 193 nm). Reasonable photosensitivity of the fiber allows writing stronger gratings within a short exposure time. The photosensitivity of the fiber core highly depends on chemical composition of the core material, UV wavelength and the irradiation intensity. A significant further improvement of photosensitivity is possible by introducing hydrogen molecules to the fiber core. This can be done by two different processes called high pressure hydrogen loading and flame brushing.

2.2.1 Hydrogen Loading

(a). High Pressure Hydrogen loading

In this method the fiber is kept inside a tube filled with gas hydrogen under a pressure in the range of *100* to *300* atmospheres for about 14 days. Due to the high pressure the Hydrogen molecules diffuse to the fiber core. Even though the process is slow and the amount of hydrogen molecules get into the fiber is less, it increases the photosensitivity of the fiber to achieve refractive index changes as high as in the range of 10^{-2} . (In general the expected refractive index change in FBG fabrication is 10^{-5} to 10^{-3}) [13].

(b). Flame Brushing

Flame brushing method takes only few minutes to increase the photosensitivity to an acceptable level with negligible signal losses in communication band. In this method, the region of the fiber to be photosensitized is brushed repeatedly with a flame fueled with hydrogen and a small amount of oxygen, having a temperature of approximately *1700* °C. At this temperature, the hydrogen diffuses to the fiber core efficiently and react with the glass to create strong absorption band, and rendering the core highly photosensitive [15].

2.2.2 FBG Fabrication Methods

There are three different grating fabrication methods, namely holographic method, point-by-point method and phase mask method.

(a). Holographic Method

In this method a UV beam is split into two at a beam splitter and then brought them together on to the fiber from side, with a mutual angle of θ , for grating inscription. The Bragg wavelength can be observed as,

$$\lambda_{bragg} = \frac{n_{eff}\lambda_{uv}}{n_{uv}\text{Sin}(\frac{\theta}{2})} \quad (2.12)$$

where, λ_{uv} is the wavelength of UV beam and n_{uv} is refractivity of silica in UV. As can be seen from Eq (2.12), Bragg wavelength can be changed from nearly λ_{uv} to infinity by changing only the value of θ while keeping the ultra violet wavelength a constant.

(b). Point-by-point method

In this technique, the region with increased photosensitivity is written point by point with a well focused small laser beam. Because of the flexibility, the method is well suited for long period Bragg grating inscription.

(c). Phase mask method

Phase mask method is the most effective method of FBG inscription and it uses a diffractive optical element to spatially modulate the UV writing beam.

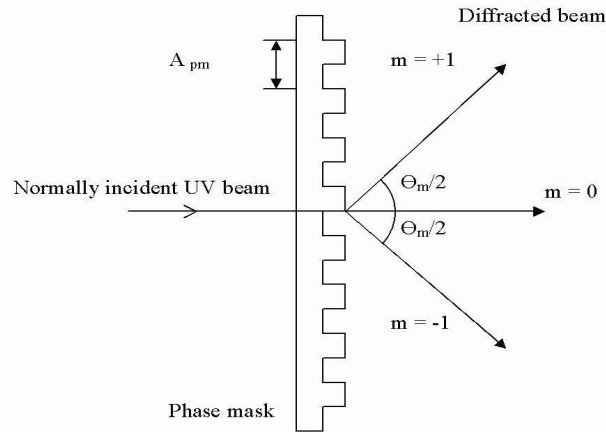


Figure 2.5: UV Radiation Over a Phase Mask with Normal Incidence

Figure 2.5 shows the UV radiation at normal incidence with diffracted radiation of $m=0$

and ± 1 orders. The interference pattern at the fiber of two beams of order ± 1 brought together as a period of the grating Λ related to the diffraction angle of $\theta_{\frac{m}{2}}$ by

$$\Lambda = \frac{\lambda_{uv}}{2\text{Sin}(\frac{\theta_m}{2})} = \frac{\Lambda_{pm}}{2} \quad (2.13)$$

where, Λ_{pm} is the period of the phase mask.

This method can be used to spatially modulate the UV writing beam as indicated in Figure 2.6.

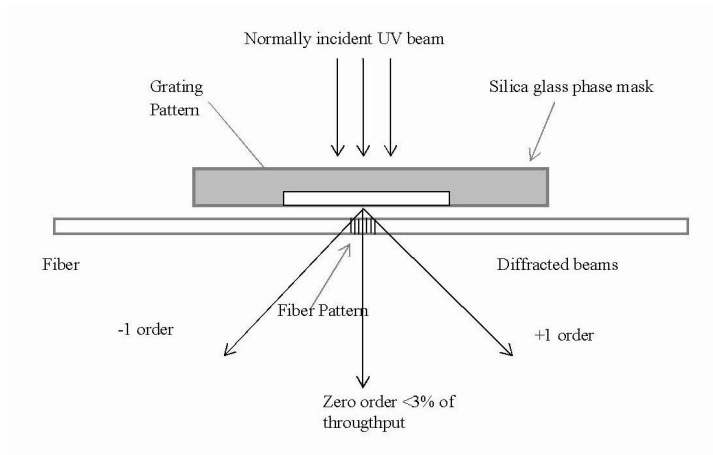


Figure 2.6: A Scheme of Phase Mask Utilized in Inscribing FBG

The structure of the periodic grating is chosen such that when the UV beam is incident on the phase mask, the zero order diffracted beam is suppressed to less than a few percent of the transmitted power. In addition to that, the diffracted ± 1 orders maximize to be about 35% of the total transmitted power. A near field fringe pattern is produced by the interference of the ± 1 order diffracted beams. The period of that fringes is one half of the mask period. The interference pattern photo-imprints a refractive index modulation in the core of the photosensitive fiber placed closer to the phase mask.

In writing the FBG, it can be apodized to reduce the side lobes of the grating spectrum. The sudden drop of strength of the index modulation in a grating from a constant level to

zero outside that range, gives side lobes and sometimes it add undesired noise to the system. Apodizing process smoothes the strength of the index modulation up and down along the grating.

2.2.3 FBG Characteristics

One of the major advantage of FBGs is the flexibility on changing spectral characteristics according to the intended application. Grating length, grating depth, induced index change and 3 dB bandwidth of the reflected or transmitted signal are some of the controllable parameters in laser inscription and these variables allow the spectral and dispersive features of the grating to be tailored.

The 3 dB bandwidth or the Full Width at Half Maximum (FWHM) of the grating can be approximated as

$$\Delta\lambda_{FWHM} \approx \lambda_{Bragg} \rho \left[\left(\frac{\Delta n}{2n_{core}} \right)^2 + \left(\frac{\Lambda}{L_g} \right)^2 \right]^{1/2} \quad (2.14)$$

where, the parameter ρ is a constant between 0.5 and 1 which depends on the reflectivity of the grating and the L_g is the grating length [13].

The reflectivity of a uniform grating can be expressed as [16]

$$R(L_g, \lambda) = \frac{\Omega^2 \text{Sinh}(SL_g)}{\Delta\beta^2 \text{Sinh}^2(SL_g) + S^2 \text{Cosh}^2(SL_g)}. \quad (2.15)$$

Here, Ω is the coupling coefficient between the forward and backward propagation modes. $\Delta\beta = 2\pi n_{eff}(\sigma - \sigma_B)$ is the phase matching parameter that defines the detuning wave vector while σ is the wave number. S is defined as $S = \sqrt{\Omega^2 - \Delta\beta^2}$.

Chapter 3

Laser Fabrication and Experimental Results

This chapter describes the process of fiber laser fabrication in detail. After that, the studies on longitudinal and orthogonal polarization modes as well as the generated microwave/radio-wave domain signals will be presented. Then, the results of Allan variance measurements, temperature and strain stability of the microwave/radio-wave signals will be presented respectively.

3.1 DBR Laser Fabrication

The short cavity DBR fiber laser designed in this thesis was fabricated on a Er/Yb co-doped fiber. Two FBGs having 99% and 90% of reflectivity at 1530 nm wavelength were used as the end reflectors. The dual wavelength operation was achieved by selecting the cavity length to 8 mm and by making the bandwidths of the FBGs sufficiently wide to reflect both modes.

Considering the gain medium of the fiber laser, it was pumped with a 980 nm pump laser. Er^{+3} ions introduced to the fiber core gives the lasing gain while, Yb^{+3} ions increasing the optical absorption at 980 nm. The Er^{+3} doped fiber core has a diameter of 4.66 μm and it is surrounded by a Yb^{3+} doped photosensitive ring with a diameter of 16 μm . The Yb^{+3} absorption at 980 nm is quoted to be ~ 2 dB/cm while the maximum Er^{+3} gain at 1530 nm is 30 dB/m.

Before FBG inscription, the Er/Yb co-doped fiber was hydrogen loaded for ten days

under a pressure of 100 atmospheres at room temperature to increase the photosensitivity. Then the phase mask method was used to write end reflector FBGs. The experimental setup used for laser inscribing is indicated in Figure 3.1

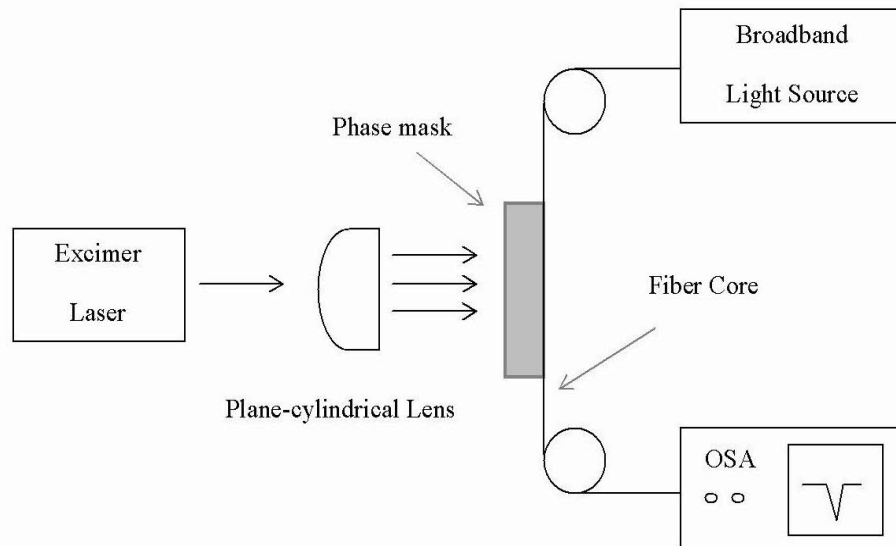


Figure 3.1: The Experimental Setup for Inscribing Bragg Gratings with a Phase Mask.

A collimated KrF excimer laser (Lumonics, Model PM844) beam was focused through a phase mask onto a horizontally positioned fiber. The typical energy density of the 248 nm pulses at the fiber is 0.05 J/mm^2 per pulse and the laser pulse rate was set to 30 Hz. The exposure time was changed according to the reflectivity needed.

The DBR laser was fabricated by direct inscription of two wavelength-matched FBGs into the active fiber. Compared to the scheme that splices two FBGs to a short length of active fiber, direct photo-writing of FBGs can provide much lower threshold because it avoids intra-cavity splice losses. Before starting FBG fabrication the active fiber was connected to a Wavelength Division Multiplexer (WDM) coupler to facilitate FBG reflectivity monitoring first and laser gain monitoring later.

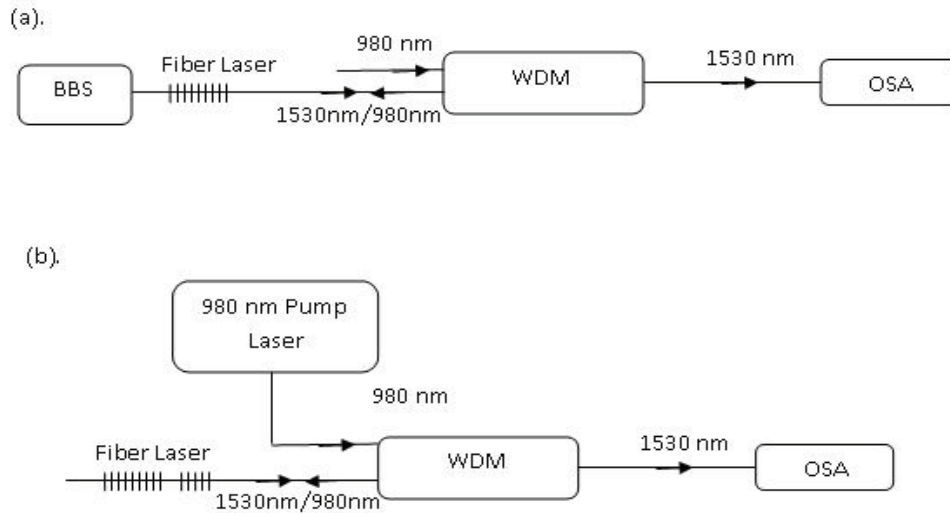


Figure 3.2: The Experimental Setup to Facilitate Laser Pumping and Gain Monitoring. (a). High Reflectivity Grating Writing (b). Low Reflectivity Grating Writing.

The high reflectivity grating was written first while monitoring the transmission spectrum of the FBG during the UV exposure by using a Broad Band Source (BBS) and an optical spectrum analyzer (OSA - Ando, model AQ-6310B). While writing the high reflectivity grating the 980 nm pump laser was switched off. 6 mm long grating with a reflectivity of 99.9% was fabricated within the exposure time of 7-8 minutes. The index profile of the FBG was apodized with a sinc function of 6 mm in length. After that the apodizing mask along with the holder was moved by 8 mm and the low reflectivity grating was written using the same phase mask. While writing the second grating BBS was turned off and the 980 nm pump laser was turned on to monitor the laser spectrum. The length of the low reflectivity grating was 2.5 mm and lasing with two longitudinal modes could be observed within an exposure time of 4-5 minutes. In this setup the WDM coupler helps to minimize the pumping losses at 980 nm and to maximize the lasing power at 1530 nm simultaneously; the insertion loss of the fiber laser output to the detector through the WDM coupler at 1533 nm is quoted to be less than 0.7 dB while that value from the pump laser to the fiber laser at 980 nm is less

than 0.32 dB. In order to achieve the wavelength matching of two FBGs with different lengths and reflectivities, the applied tension over the fiber was changed accordingly; a tension of about 0.3 N was applied over the fiber while writing the high reflectivity grating and about 0.2 N while writing the low reflectivity grating. Later the DBR laser was annealed at 150 °C for over 15 hours to ensure the long term stability of FBGs.

3.2 Optical Features of the Fiber Laser

The measured transmission spectrum of two FBGs after annealing is indicated in Figure 3.3. Reducing the 3 dB bandwidth of FBGs while achieving a high reflectivity as 30 dB is always a challenge. Even though the high reflectivity FBG supports around 6 FBG modes, only two modes came up with lasing due to mode competition.

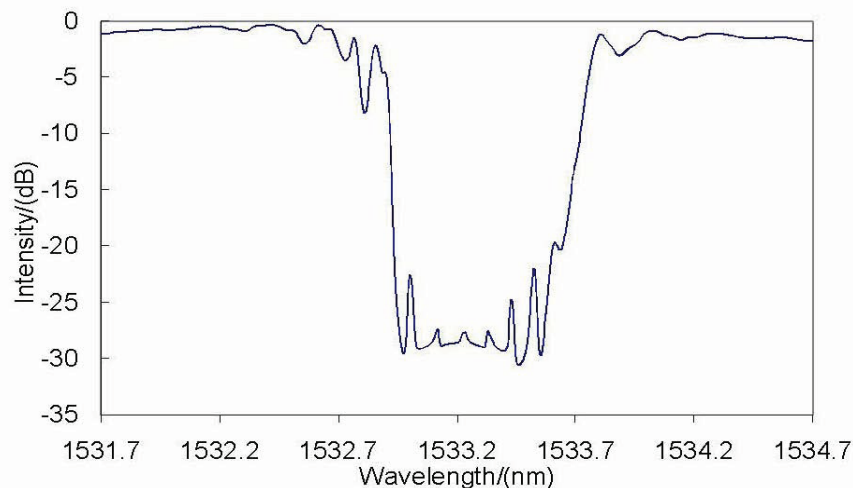


Figure 3.3: The Transmission Spectrum of Two FBGs After Annealing.

The optical transmission spectrum shown in Figure 3.3 is different from a transmission spectrum of a regular FBG due to its relatively flat bottom. This can be realized when considering the overlapping of transmission effects of high reflectivity grating over that of low reflectivity grating.

3.2.1 Dual Longitudinal Mode Operation

The OSA with resolution of 10 pm was used to monitor the laser spectrum. Two longitudinal laser modes were observed at 1533.72 nm and 1533.84 nm with a separation of 120 pm which corresponds to the cavity length of 8 mm. The optical signal-to-noise ratio of the laser was approximately 70 dB.

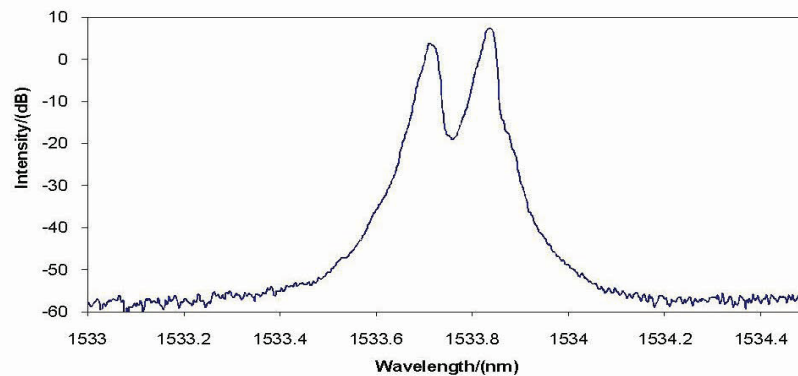


Figure 3.4: Dual Longitudinal Mode Operation of the Short Cavity Fiber Laser.

As can be seen from the Figure 3.4, the 3 dB bandwidth of each longitudinal laser mode was measured to be 27.5 pm. The shape of the curve is limited by the resolution of the OSA and hence the actual 3 dB bandwidth can be less than the measured value.

3.2.2 Orthogonal Polarization Modes

Due to the fiber birefringence introduced during laser fabrication it was observed that, each longitudinal mode contains two orthogonal polarization modes. The frequency separation $\Delta\nu$ between these polarization modes is given by

$$\Delta\nu = \frac{B\nu}{n} \quad (3.1)$$

where ν is the lasing frequency, B and n are the birefringence and the refractive index of the fiber respectively. These two orthogonal polarization modes, couldn't be observed during the regular OSA measurements because the wavelength separation is less than the resolution of the instrument. So in order to measure the polarization modes accurately two different approaches were used.

Transmission Spectrum analysis

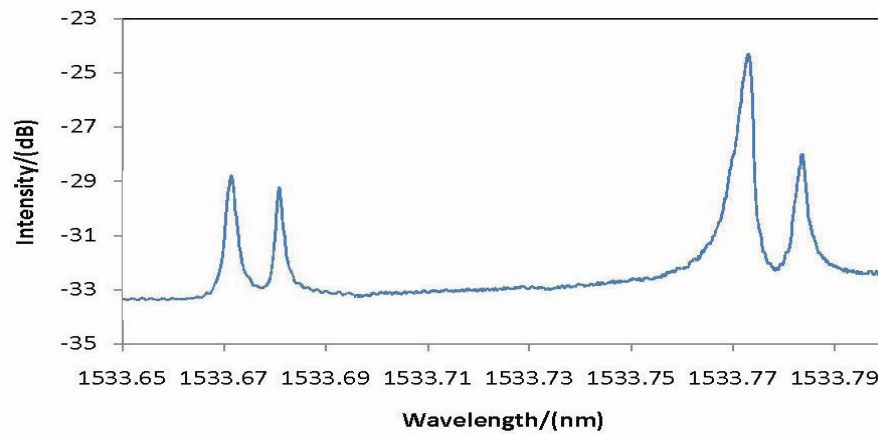


Figure 3.5: Orthogonal Polarization Modes in Each Longitudinal Mode - Transmission Spectrum Analysis.

The transmission spectrum of the laser cavity with two FBG end reflectors was measured using a Tunable Laser (Agilent 8164A). The resolution of the measuring device was set at 1 pm. The observed two orthogonal polarization modes in each longitudinal mode have indicated in Figure 3.5. Wavelength separation between two polarization modes was measured to be 9 pm. Considerable intensity difference between two longitudinal modes having a wavelength separation of 120 pm is apparent when considering the shape of the combined transmission spectrum of FBGs.

Laser Spectrum Analysis

In order to observe the two orthogonal polarization modes, the lasing output was monitored with a Fabry-perot Interferometer (Burleigh Highpase Etalon system). The sensitivity of the instrument was 150 MHz which is acceptable to measure a wavelength separation less than 10 pm. The detected signal from the interferometer was monitored with a regular oscilloscope (Tectronix, TDS 3054B).

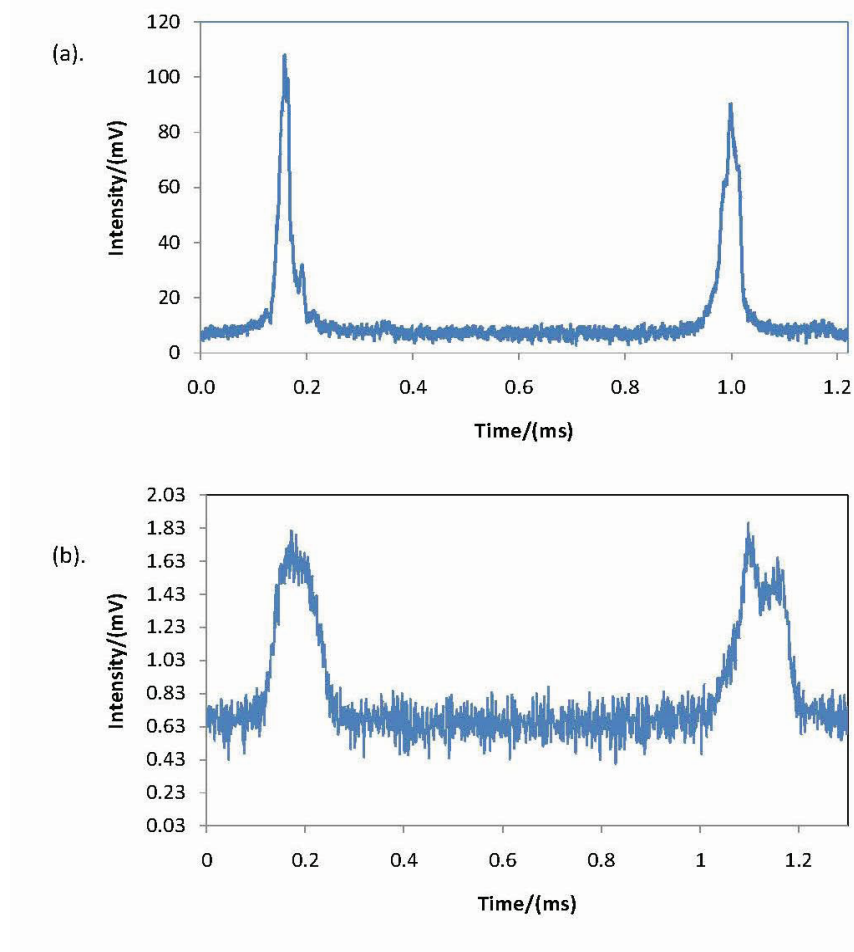


Figure 3.6: (a). Calibrating Signal. (b). Two Longitudinal Laser Modes with Two Orthogonal Polarization Modes.

First the system was calibrated by using two known laser signals. The wavelengths of two DFB lasers (E-Tek tunable laser, tunability of 10 pm in wavelength) were measured with a Wave Meter (Hewlett Packard - 86120 B) having an accuracy of 1 pm as 1556.000 nm and 1556.120 nm (i.e. a separation of 120 pm). The combined signal gave a 880 μ s separation on the oscilloscope as shown in Figure 3.6-(a).

Then the spectrum of the new DBR laser was measured without changing the configurations of the etalon system (i.e without changing the mirror separation, scan duration and the amplitude). The two longitudinal modes of the laser as well as the polarization modes could be observed. In order to improve the SNR of the total system, an EDFA was used. The maximum SNR, without saturating the overall system could be achieved with EDFA current of 129 mA.

Here the wavelength separation of the two longitudinal laser modes is about 880 μ s which corresponds to about 120 pm, matching with the wavelength measured with the OSA. The separation of polarization modes in each longitudinal mode was 70 μ s in time and corresponded approximately to 9 pm in wavelength.

3.3 Microwave and Radio-Wave Signal Generation

The short cavity fiber laser was used to generate microwave and radio-wave signals by beating its output on a fast photo-detector (Tektronix OI 2125 O/E Receiver). Generated electrical domain signals were monitored with a Wireless Communication Analyzer (WCA-Tektronix 380) that measures microwave signals up to 3 GHz and a microwave spectrum analyzer (Hewlett Packard-8564 E) that measures up to 40 GHz. Four microwave signals at 1.2687 GHz, 1.2828 GHz, 14.6962 GHz and 14.7103 GHz as well as a radio-wave signal at 14.1 MHz were observed.

3.3.1 Microwave Signals at 1.2687 GHz and 1.2828 GHz

Due to the beating effect of two orthogonal polarization modes (having a wavelength separation of 9 μm) in each longitudinal mode, two microwave signals at 1.2687 GHz and 1.2828 GHz were observed with a frequency separation of 14.1 MHz.

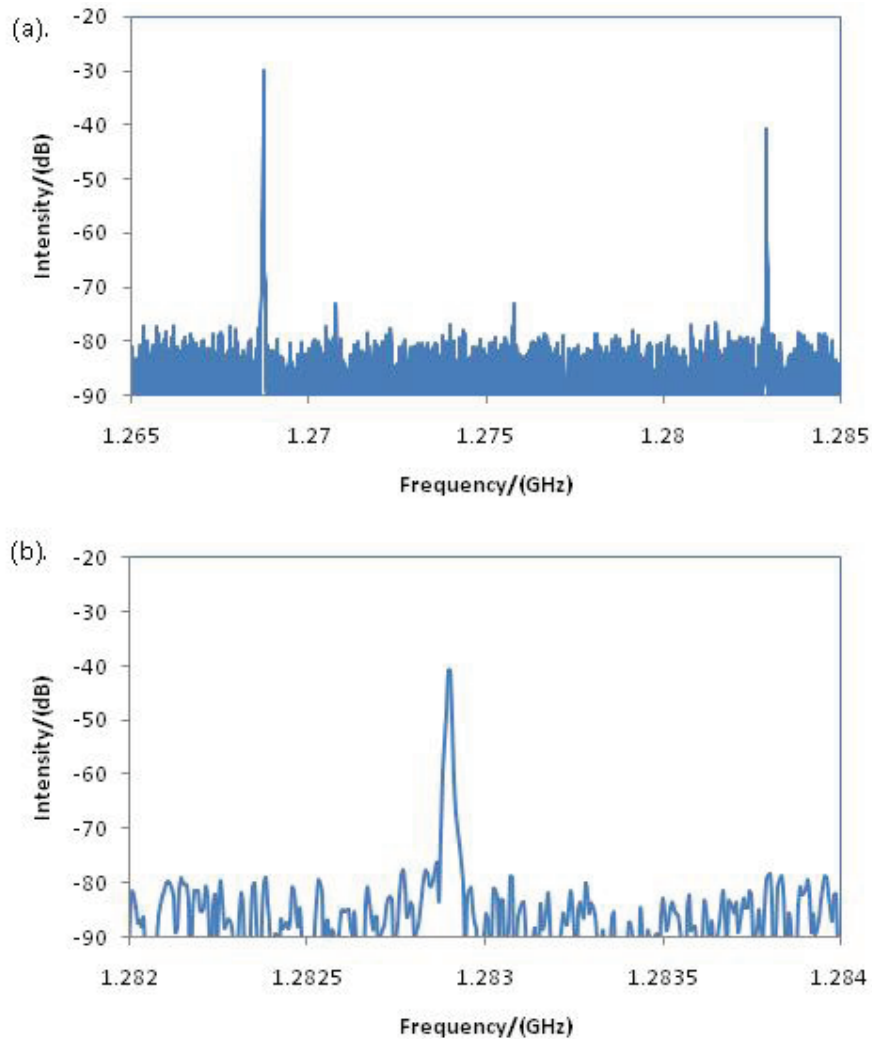


Figure 3.7: (a). Microwave Signals Generated at 1.2687 GHz and 1.2828 GHz. (b). Zoomed Signal at 1.2828 GHz

The 3 dB bandwidth of these two microwave signals were measured to be 15.25 kHz and 12.5 kHz respectively with a resolution of 6.25 kHz at the WCA. The zoomed signal at

1.2828 GHz has indicated in Figure 3.7. The actual 3 dB bandwidth of the generated signals could be less than the measured values, and it is limited by the resolution of the measuring instrument. The SNR of the signals observed to be higher than 45 dB.

3.3.2 Microwave Signals at 14.6962 GHz and 14.7103 GHz

In addition to 1.2687 GHz and 1.2828 GHz microwave signals, two more microwave signals at 14.6962 GHz and 14.7103 GHz were also observed. These are shown in Figure 3.8 and are correspond to the beating of two longitudinal modes having a wavelength separation of 120 pm. Again the frequency separation of two signals was 14.1 MHz, which is similar to the frequency separation of two microwave signals at 1.2 GHz.

The 3 dB bandwidth of two signals was measured with a resolution of 7 kHz at the microwave spectrum analyzer, and it was observed to be 33.33 kHz and 40 kHz respectively. The SNR of the signals were higher than 45 dB.

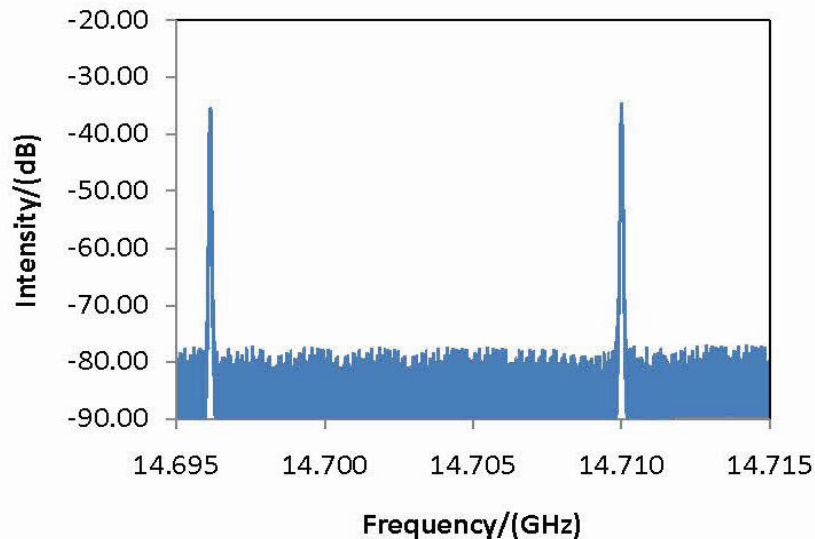


Figure 3.8: Microwave Signals Generated at 14.6962 GHz and 14.7103 GHz.

3.3.3 Radio-Wave Signal at 14.1 MHz

As discussed above, two microwave signals at 1.2687 GHz and 1.2828 GHz as well as two microwave signals at 14.6962 GHz and 14.7103 GHz with frequency separation of 14.1 Mhz was generated, by beating of different laser modes. Another radio-wave signal at 14.1 MHz with a SNR of 30 dB also observed due to the beating of generated microwave signals as shown in Figure 3.9. The 3 dB bandwidth was measured to be 9.375 kHz.

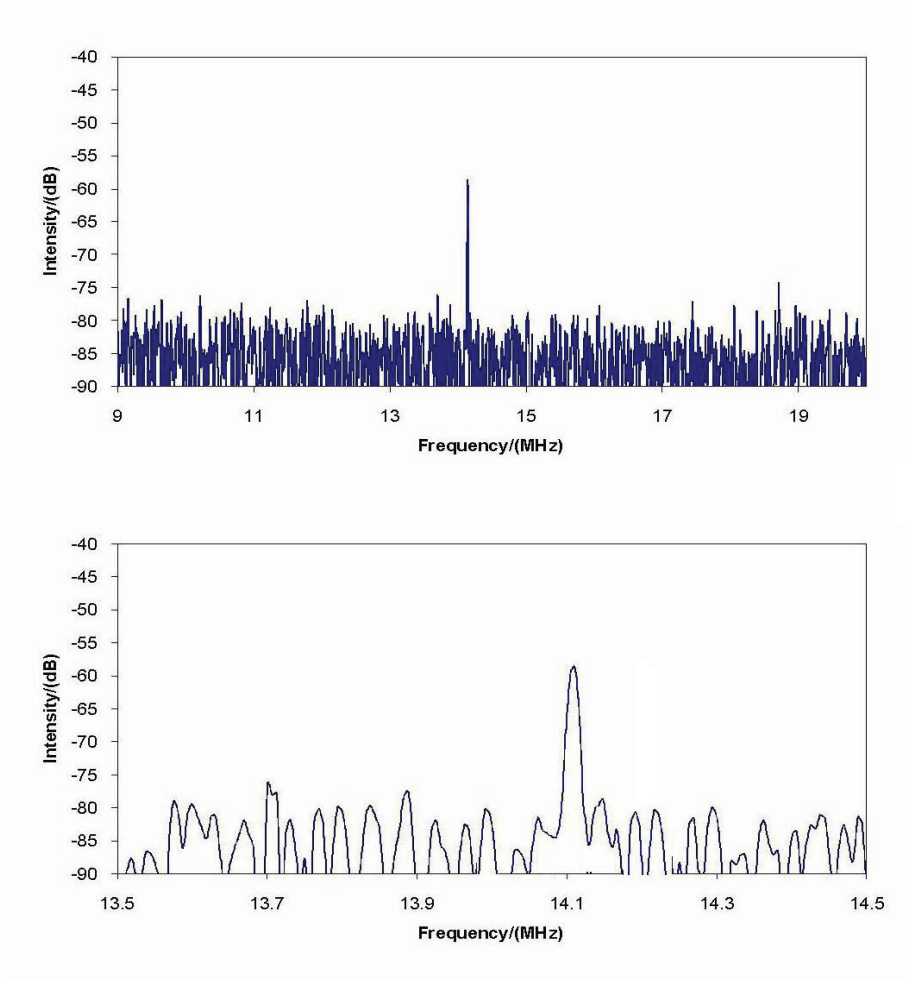


Figure 3.9: (a).The Radio-Wave Signal Generated at 14.1 MHz. (b). Zoomed Signal.

Only one radio-wave signal was observed at 14.1 MHz, with a resolution of 6.25 kHz at the WCA. So it is apparent that the beating effects of two sets of microwave signals at 1.2 GHz and 14.6 GHz are identical each other.

3.3.4 Beating Effects and 3 dB Bandwidth of Millimeter Waves

In order to understand the beating effect of generated signals, the generated laser modes can be named as follows; the two orthogonal polarization modes in first longitudinal mode as $f_{a,\perp}$ and $f_{a,\parallel}$ and the two orthogonal polarization modes in second longitudinal mode as $f_{b,\perp}$ and $f_{b,\parallel}$. The beating effect corresponds to each microwave and radio-wave frequency signal has summarized in Table No. 3-1.

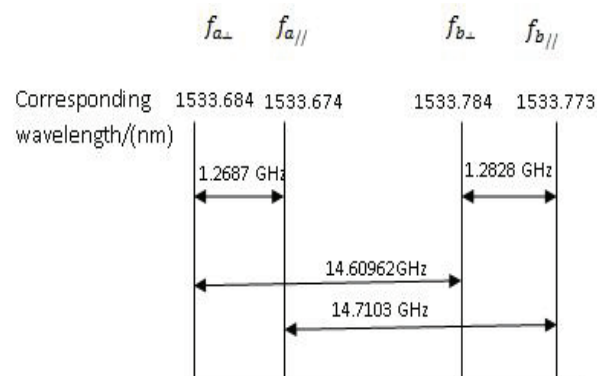


Figure 3.10: Approximated Diagram of Different Modes of the Short Cavity Fiber Laser in Frequency Domain.

As can be seen from Figure 3.6 two polarization modes in each longitudinal mode are not identical each other and because of that there is a difference of 14.1 MHz among the polarization mode separation in frequency domain.

Table No. 3-1: Beating Effects corresponds to generated Microwave radio-wave Signals

Frequency/(GHz)	Beating Effect	3 dB bandwidth/(kHz)
1.2687 GHz	$(f_{a, //} - f_{a, \perp})$	15.25
1.2828 GHz	$(f_{b, //} - f_{b, \perp})$	12.5
14.6962 GHz	$(f_{a, //} - f_{b, //})$	36.33
14.7103 GHz	$(f_{a, \perp} - f_{b, \perp})$	40
14.1 MHz	$(f_{b, //} - f_{b, \perp}) - (f_{a, //} - f_{a, \perp})$ or $(f_{a, \perp} - f_{b, \perp}) - (f_{a, \perp} - f_{b, \perp})$	9.38

The measured 3 dB Bandwidths of all four microwave signals and radio-wave signal were observed to be less than 40 kHz as indicated in Table No 3-1. During the measurements we observed that the measured value of the 3 dB bandwidth is limited by the resolution of the WCA or microwave spectrum analyzer. Hence the actual 3 dB bandwidth of the generated signals should be less than 40 kHz.

3.4 Stability Measurements

In order to analyze the stability of the generated microwave and radio-wave signals, Allan variance was measured to determine the frequency stability of the generated signals. The frequency was also measured as a function of temperature and strain to determine the environmental impact on the generated signals.

3.4.1 Allen Variance Measurements.

The Allan Variance is a method of analyzing a time sequence to pull out the intrinsic noise in the system as a function of the averaging time [17]. It was developed for clocks, but can be easily adapted for other types of outputs as well.

The variation of the each signal with time was observed by using the Wireless Communication Analyzer for different averaging time called the bin period as indicated in Figure 3.11.

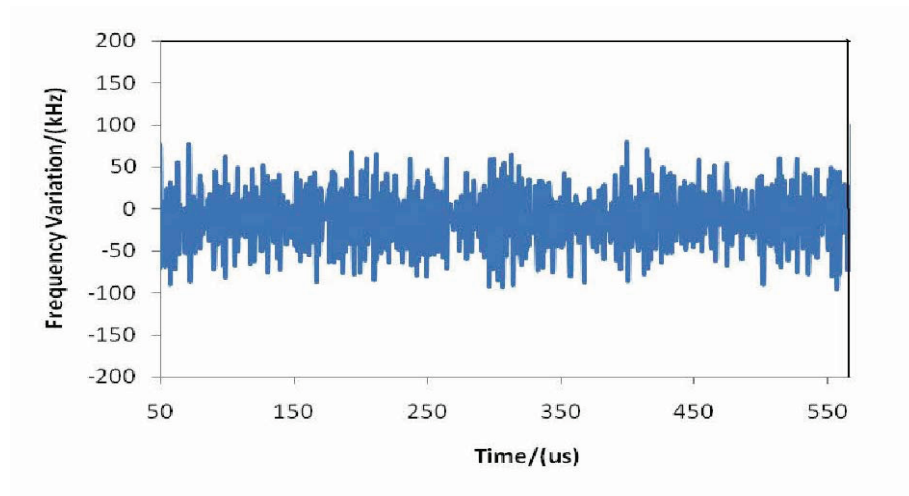


Figure 3.11: Frequency Variation at averaging time of $0.625\mu s$.

Figure 3.11 shows that the frequency variation of the signal is about 150 kHz with averaging time of $0.625 \mu s$. To calculate the Allan Variance, we took the difference in frequency between successive bins, squared this number, added them all up, and divided by a rescaling factor. Mathematical expression for this procedure can be indicated as follows [17]:

$$AVAR^2(\tau) = \frac{1}{2(n-1)} \sum [y(\tau)_{i-1} - y(\tau)_i] \quad (3.2)$$

where, $AVAR(\tau)$ is the Allan variance as a function of the averaging times, τ ; y_i is the average value of the measurement in bin i and n is the total number of bins.

Same procedure was followed with different averaging times to get at least 6 points in Allan variance curve. Because we didn't have a standard frequency counter, same WCA was used to measure the signal frequency variations in time domain. Due to the instrument limitations, the bin period was changed by changing the frame rate of the instrument.

Figure 3.12, Figure 3.13 and Figure 3.14 indicate the Allan variance plots in log-log scale for two microwave signals at 1.2 GHz and the Radio wave signal at 14.1 MHz.

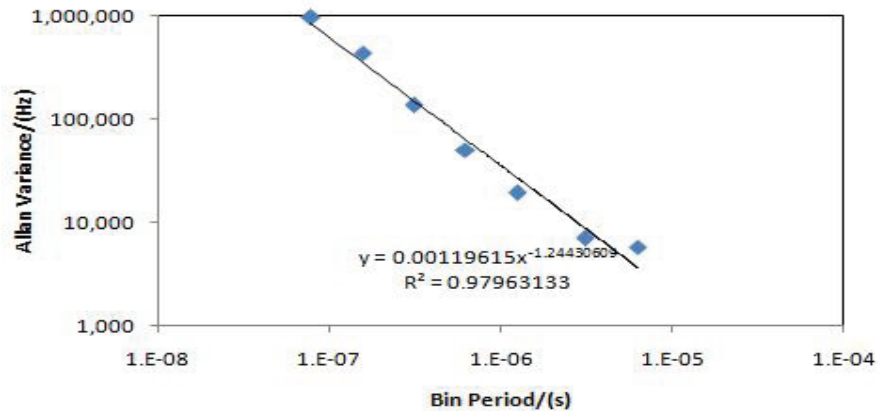


Figure 3.12: Plot of Allan Variance of the 1.2687 GHz Signal.

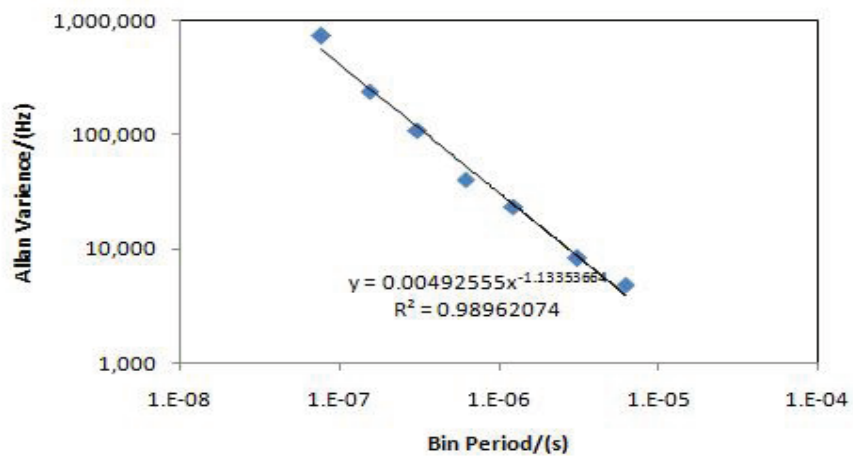


Figure 3.13: Plot of Allan Variance of the 1.2828 GHz Signal.

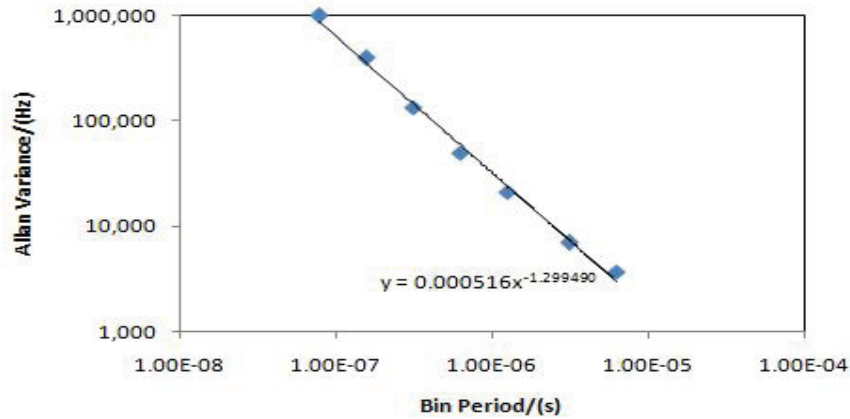


Figure 3.14: Plot of Allan Variance of the 14.1 MHz Signal.

According to the power law, a common frequency domain modal for the spectrum $S(w)$ of a low frequency time series is given by

$$S(w) = a\tau^\alpha \quad (3.3)$$

where α is the slope of the log-log spectrum. According to the power-law model, there are five types of noise processes namely random walk frequency noise, flicker frequency noise, white frequency noise, flicker phase noise and white phase noise, with α equals to -2, -1, 0, +1, and +2 respectively [17]. There is a one-to one correspondence between α and the slope of the Allan variance plot as indicated in Table 3-2.

Table No. 3-2: Relationship between noise processes and slope of the Allan variance plots.

Noise modal	Slope of the power spectrum (α)	Slope of the Allan variance plot $(-\alpha-1)/2$
Random walk	-2	0.5
Flicker noise	-1	0
White noise	0	-0.5
Flicker phase	1	-1
White phase	2	-1.5

Since the slopes of Allan variance curves observed during the experiments are closer to -1.5 in all cases, the frequency variation of generated microwave and radio-wave signals are near the white phase noise limit.

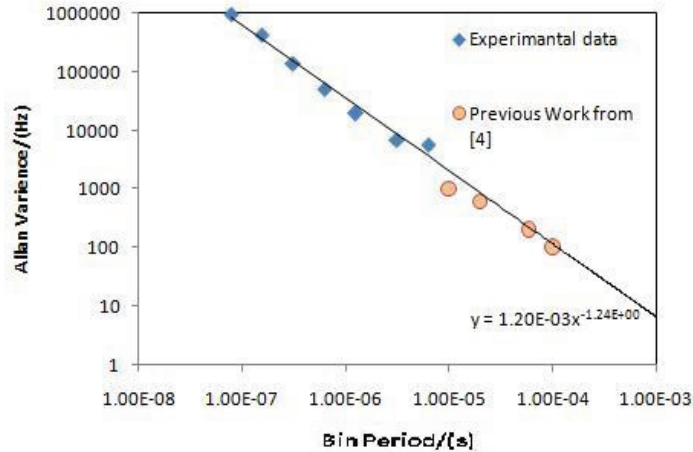


Figure 3.15: Comparison of Frequency Stability with Previous Work Reported.

In order to compare the stability of the generated signals, with the previous works, we considered the allan variance results in [4] as depicted in Figure 3.15. In [4], J. Geng and his group have calculated the allan variance of the microwave signals at 1 GHz, which was generated by using a Dual frequency Brillouin fiber laser. The figure shows that the generated signals using the short cavity fiber laser has similar stability as [4], and hence few hertz of frequency stability with an averaging time of few seconds can be grated by forward forecasting the observed curves.

3.4.2 Temperature Dependency Measurements

In order to understand the temperature stability of the generated microwave and radio-wave signals, they were measured with changing temperatures. To change the temperature of the fiber laser it was placed inside a chamber of temperature controller (Thorlabs-TC 200) and the beat notes were measured of different temperatures with a step size of 10 °C.

Observed results of two 1.2 GHz microwave signals as a function of temperature are plotted in Figure 3.16.(a) and Figure 3.16.(b).

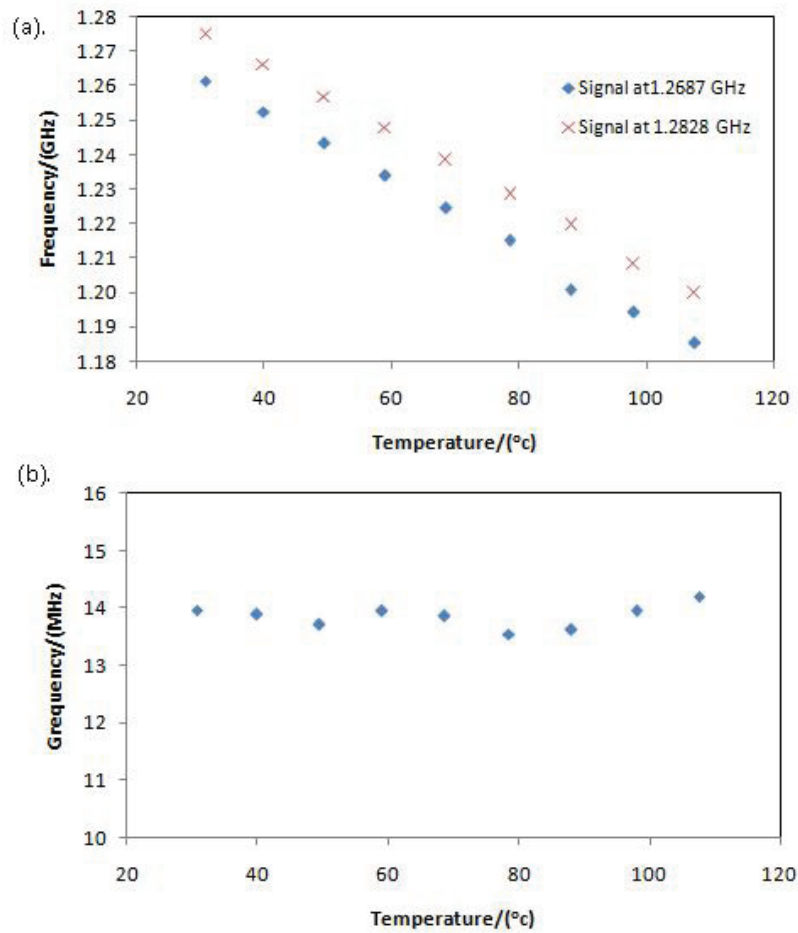


Figure 3.16: (a).Frequency Variation of the Two Microwave Signals at 1.2687 GHz and 1.2828 GHz with Temperature. (b). Frequency Variation of the Radio-Wave Signal at 14.1 MHz with Temperature.

According to Figure 3.16.(b) the frequency of generated radio-wave signal varies by $\pm 250\text{kHz}$ when changing the temperature from 23°C to 110°C ; so it is reasonably stable in temperature. But the generated microwave signals indicate a linear relationship with temper-

ature, a feature that can be used for temperature sensing. Since the gradients of two curves of Figure 3.16 similar to each other with a value equals to 1 MHz/celsius, the radio-wave signal generated by beating of microwave signals shows a higher stability in temperature. Also it denotes that all four polarization modes generated by the short cavity fiber laser demonstrate a identical variation with temperature.

3.4.3 Strain Dependency Measurements

It is well known that the characteristics such as Bragg wavelength of FBGs vary with the applied tension. Therefore, to understand the behavior of generated millimeter wave signals, the beat note output wave measured using the a microwave spectrum analyzer as a function of applied tensions.

One end of the fiber laser pigtail was clamped to an optical table and a known weight was applied over the other end by using a hook.

Considering the definition of the elastic modulus, the micro strain ϵ can be written as

$$\epsilon = \frac{mg}{A\lambda} \quad (3.4)$$

where m is the applied mass measured in grammes, A is the cross section area of the fiber measured in millimeter squared and the λ is the elastic modulus in Gigapascals. For a typical fiber λ equals to 72.5 GPa and A can be considered as 0.0123 mm^2

The observed results are shown in Figure 3.17.(a) and Figure 3.17.(b) and they indicate that the generated microwave and radio-wave signals linearly depend on the applied strain over the fiber laser.

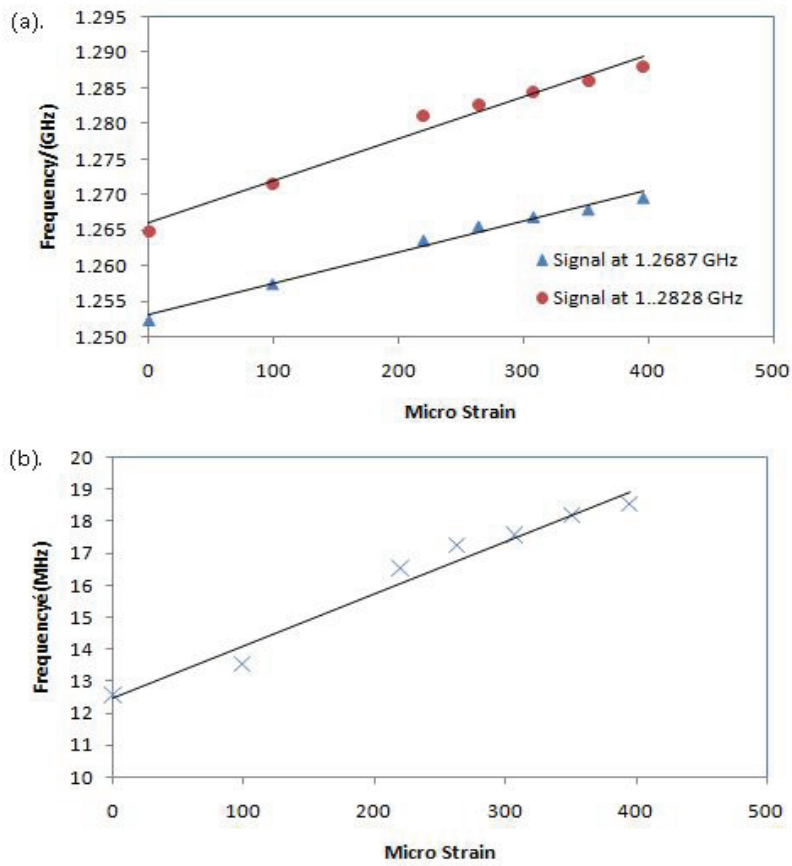


Figure 3.17: (a).Frequency Variation of Two Microwave Signals at 1.2687 GHz and 1.2828 GHz with Micro Strain. (b).Frequency Variation of Radio-Wave Signal at 14.1 MHz with Micro Strain

Chapter 4

Discussion and Future Works

This chapter details the potential applications of the fiber laser, other than the microwave and radio-wave signal generation, such as optical clockworks and measuring of ultrasound, temperature as well as strain.

4.1 Possible Other Applications

4.1.1 Optical Clockwork

Optical clock uses the high frequency optical signals to generate the periodic signal which is required for any kind of clock. Due to the high frequency of optical signals as high as 10^{15} Hz, optical clocks enable to count the oscillation in fraction of 1 fs. Other than that optical clock has the following advantages compared to the microwave standards like in atomic clock.

- There are certain atoms and ions with extremely well defined clock transitions which promise higher accuracy and stability than the best microwave atomic clocks. The relative frequency uncertainty of the optical clock is of the order of 1×10^{-18} while the uncertainty of Cs clock is in the order of 1×10^{-15} [18].
- Since the oscillations are in optical domain, the benefits in optical transmission systems can be adopted easily.

However, counting oscillations having such a high frequency is always a challenge. In response to this challenge, optical clockworks have been introduced, which are capable of

down converting optical frequency oscillations into microwave domain as in Cesium atomic clock. When considering the state-of-the-art techniques, S.A.Diddams *et al.* have introduced a femto-second laser-based clockwork to down convert the optical frequency into countable microwave frequency [18]. The optical frequency has been coherently divided down by using a mode-locked femto-second laser along with microstructure optical fiber. Another optical clockwork with an offset-free difference-frequency comb, has been demonstrated in [19]. All these methods involve complicated optic setup and have limitations of high of component costs.

As explained in Chapter 3 the short cavity fiber laser introduced in this thesis is capable of down converting the optical frequencies into microwave and further into radio-wave domain. This feature can be used to develop optical clockworks. According to the Allan variance measurements, the generated microwave and radio-wave signals have a high frequency stability and can be improved further by employing mode locking. Also the high temperature stability of the generated radio-wave signal makes the short cavity fiber laser, a good candidate for optical clockworks.

4.1.2 Measuring Ultrasound Signals

The increasing sophistication of ultrasonic techniques for medical ultrasound has developed an increasing concern for precise measurements of the ultrasound dosage for safety reasons. It is of great interest to study not only the acoustic field distribution, but also the absolute value of the acoustic pressure amplitude generated by the diagnostic ultrasound equipment. Because excessive acoustic output may lead to undesirable biological effects. Hence, considerable effort has been put into the development of high performance Hydrophones.

The short cavity, single longitudinal mode fiber laser in [9]-[11], similar to what in this thesis, has been used to measure ultrasound frequencies. The frequency and the amplitude of the ultrasound signal can be measured by modulating the generated microwave signal with it. The frequency difference of side bands gives the frequency while the amplitude indicates the strength of the measured ultrasound signal.

4.1.3 Temperature Sensing

According to the temperature stability measurements of the generated microwave signals, approximately 1 MHz frequency variation for each 1 °C change in frequency is observed. This linear relationship of generated microwave signal frequency with temperature enables using the short cavity fiber laser in temperature sensing.

4.1.4 Strain Measurements

As can be seen from Figure 3.17 and Figure ?? the generated microwave and radio-wave signals have a linear relationship with applied tension. Hence, the short cavity fiber laser introduced in this thesis can be used in strain measuring systems. The sensitivity can vary with the selected microwave or radio-wave signal; high strain sensitivity can be achieved when using the microwave signals at 1.2 GHz than using of radio-wave signal at 14.1 MHz in strain measurements.

4.2 Conclusion

The primary goal of this thesis was to generate microwave and radio-wave signals by using a Er/Yb co-doped short cavity fiber laser. A DBR fiber laser was fabricated with a cavity length of 8 mm by directly photo-writing the FBGs into the gain medium. Two stable longitudinal modes were observed with a separation of 120 pm in wavelength which corresponds to the cavity length of the fiber laser. Two orthogonal polarization modes in each longitudinal mode having a 9 pm wavelength separation were visualized.

Optical heterodyning method was used to generate millimeter wave signals. Microwave signals at 1.2687 GHz/1.2828 GHz and 14.6962 GHz/14.7103 GHz as well as a radio-wave signal at 14.1 MHz were generated by beating the two longitudinal laser modes and orthogonal laser modes on a photo-detector.

The 3 dB bandwidth of the generated signals were measured to be less than 40 kHz. The frequency stability of the millimeter wave signals were verified using Allan variance measurements. Forward forecasted results of Allan variance shows that the frequency variation of the

generated signals could be few hertz when the averaging time is longer than 10 seconds. It is evident that the generated radio-wave signal is reasonably stable in temperature. According to results observed in section 3.4 the generated microwave signals depict a linear relationship of 1 MHz/ $^{\circ}$ C which enables the laser to be used in temperature sensing.

4.3 Future Works

In the experiment, the cavity length of the laser was fixed to 8 mm. The frequency of the generated microwave signal at 14.6 GHz corresponds to this cavity length. and Microwave signals with different frequencies can be generated by changing the cavity length of the fiber laser. The microwave signal generated at 1.2 GHz and the radio signal generated at 14.1 MHz depend on the orthogonal polarization modes. So changing of the frequencies of these signals is limited because of the limitations of changing the birefringence of the gain medium as well as the FBGs.

Because of the instrumentation limitations, the Allan variance was forward forecasted to understand the frequency stability of the generated signals with higher averaging times. This can be eliminated by using a high frequency counter to get the frequency variations with higher averaging times as several seconds.

The experimental procedure described in this thesis is limited to generation of microwave and radio-wave frequencies which can be used in RoF and MOF systems. So in future, the generated radio-wave capable optical carrier can be modulated with a data signal and can be transmitted over fiber to realize data communication links.

Bibliography

- [1] J. Genest, M. Chamberland, P. Tremblay and M. Tetu. “Microwave signals generated by optical heterodyne between injection-locked semiconductor lasers” *IEEE Journal of Quantum Electronics*, vol. 33, no 6, June 1997.
- [2] J. Harison, and A. Mooradian “Linewidth and offset frequency locking of external cavity GaAlAs lasers.” *IEEE Journal of Quantum Electronics.*, vol. 25, no 6, June 1989.
- [3] Z. F. Fan, and M. Dagenais “Optical generation of a mHz-linewidth microwave signal using semiconductor lasers and a discriminator-aided phase locked loop.” *IEEE Transactions on Microwave Theory and Techniques.*, vol. 45, no 8, August 1997.
- [4] J. Geng, S. Staines, and S. Jiang “Dual frequency Brillouin fiber laser for optical generation of tunable low-noise radio frequency/microwave frequency.” *Optics Letter.*, vol. 33, no 1, 1 January 2009.
- [5] J. J. O’Reilly and P. M. Lane. “Remote delivery of video services using mm wave and optics.” *Electron. Letters*, vol. 28, no 25, June 1992.
- [6] J. Yu, Z. Jia, L. Yi, Y. Su, G. Chang and T. Wang “Optical millimeter-wave generation or up-conversion using external modulators.” *IEEE Photonics Technology Letters*, vol. 18, no 1, January 2006.
- [7] X. Chen, Z. Deng, X. L. Zhang and J. Yao “Photonic generation of microwave signal using a dual-wavelength single-longitudinal-mode fiber ring laser.” *IEEE Transaction on Microwave Theory and Techniques.*, vol. 54, no 2, February 2006.

- [8] G. J. Chen, D. X. Huang, X. L. Zhang, H. Hui and W. C. Chen “A proposal and demonstration for photonic generation of microwave signals by incorporating a microring resonator.” *Chinese Physics Letters.*, vol. 26, no 3, 2009.
- [9] B. O. Guan, H. Y. Tam, S. T. Lau, and H. L. W. Chan, “Ultrasonic hydrophone based on distributed bragg reflector fiber laser” *IEEE Photonics Technology Letters*, vol 16. no 1, January 2005.
- [10] B. O. Guan, H. Y. Tam and Y. Zhang “Ultra-short distributed bragg reflector fiber laser for sensing applications.” *Optics Express* 10050, vol 17. no 12, 8 June 2009.
- [11] B. O. Guan, H. Y. Tam and Y. Zhang “Fiber grating laser sensors.” *International Conference on Advanced Information technology.*, 29-31 July 2008, Shenzhen, China.
- [12] B. O. Guan, H. Y. Tam and Y. Zhang “Analytical model for rare-earth-doped fiber amplifiers and lasers.” *IEEE Journal of Quantum Electronics.*, vol 30. no 8, August 1994.
- [13] Kenneth O. Hill and G. Meltz. “Fiber bragg grating technology fundamentals and overview.” *Journal of Lightwave Technology*, vol. 15, no 8, August 1997.
- [14] S. suchat and P. P. Yupapin. “A phase mask fiber grating and sensing applications.” *Songklanakarin J.Sci. Technology.*, 2003,25(5).
- [15] F. Bilodeau, B. Malo, J. Albert, D. C. Johnson, K. O. Hill, Y. Hibino, M. Abe and M. Kawachi. “Photosensitization of optical fiber and silica-on-silicon/silica waveguides.” *Optics Letters.*, vol. 18, no 12, 1993.
- [16] A. Othonos. “Fiber Bragg gratings.” *Review of Scientific Instruments.*, vol. 68, issue 12, pp. 4309-4341, December 1997.
- [17] N. El-Sheimy H. Hou and X. Niu. “Analysis and modeling of inertial sensors using Allan Variance.” *IEEE Transactions on Instrumentation and Measurements.*, vol. 57, No 1, January 2008.

- [18] S. A. Diddams, Th. Udem, J. C. Bergquist, E. A. Curtis, R. E. Drullinger, L. Hollberg, W. M. Itano, W. D. Lee, C. W. Oates, K. R. Vogel and D. J. Wineland. “An optical clock based on a single trapped $^{199}\text{Hg}^+$ Ion.” *Journal of lightwave technology*, vol. 15, no 8, August 1997.
- [19] M. Zimmermann, C. Gohle, R. Holzwarth, T. Udem and T. W. Hansch. “Optical clockwork with an offset-free difference-frequency comb: accuracy of sum- and difference frequency generation.” *Optics Letters*, vol. 29, no 3, 1 February 2004.
- [20] D. Mathoorasing and C. Kazmierski. “Millimeter wave optical source intended for a distribution network of radio over fiber type.” *United State Patant.*, Patent Number: 6,111,678, 29 August 2000.
- [21] J. Yao “Microwave photonics.” *Journal of lightwave technology*, vol. 27, no 3, 1 February 2009.
- [22] G. Keiser. “Optical fiber communications.” *Thired Edition*, Chapter 01, 02 and 04.